SUPERCOLLIDER PHYSICS: A PROSPECTUS

C. QUIGG
Fermi National Accelerator Laboratory
P. O. Box 500, Batavia, Illinois 60510

ABSTRACT

These six lectures are devoted to a summary of the motivation for exploring the 1 TeV scale and to a review of the new phenomena that may await us there. The topic treated include the consequences of the standard model, as well as extensions to the conventional picture.

LECTURE 1: PRELIMINARIES

In these lectures I shall discuss the physics issues that lead us toward the exploration of the 1 TeV scale and which, in more general terms, impel us toward the construction of a high-energy, high-luminosity hadron collider, or "supercollider." The treatment given here is self-contained, but necessarily selective, and can only serve as a short introduction to the subject. Although thinking about supercollider physics has only been focussed for about three years, the literature is already vast. Much of what I will have to say is based on the survey by Eichten, Hinchliffe, Lane, and myself,[1] otherwise known as *EHLQ*. Some other useful general references are collected in Ref. 2.

In this opening lecture, I will briefly review the status of the standard model of particle physics, and indicate some of the ways in which it is incomplete or otherwise unsatisfactory. Then I will recall the arguments for new physics on the 1 TeV scale – we shall return to these in more detail in later lectures – and comment on the possibilities for experimental study of that regime. The main business of this lecture is to recall the methods of the renormalization group improved parton model for the calculation of cross sections for hard-scattering reactions, and to discuss what needs to be known about parton distributions in order to make possible reliable estimates of rates for processes to be studied with a supercollider.

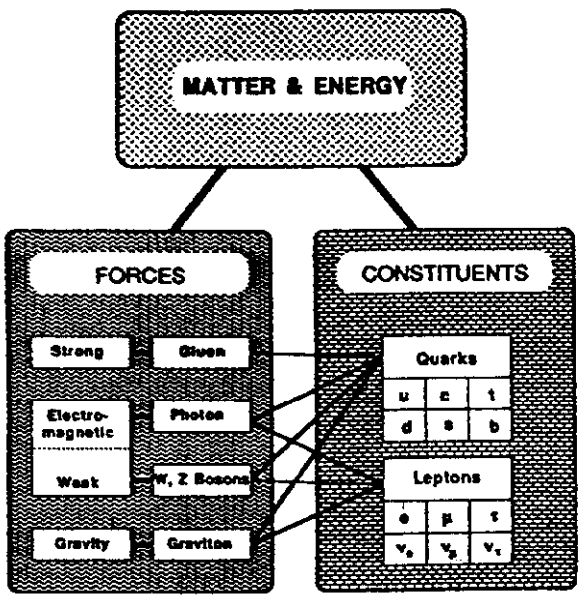

Figure 1: The Standard Model of Particle Physics.

1.1 WHERE WE STAND

The Standard Model is shown schematically in Fig. 1. It is, at least at first sight, a scheme of considerable economy. We have identified a small number of fundamental constituents, the quarks and leptons, and have recognized that the elementary interactions among them all may be described by gauge theories. The picture has a pleasing degree of coherence, and holds the promise of deeper understanding – in the form of a further unification of the elementary interactions – still to come.

This is an accomplishment worthy of the pleasure we take in it, but if we have come impressively far in the past fifteen years, we still have quite far to go. The very success of the standard $SU(3)_c \otimes SU(2)_L \otimes U(1)_Y$ model prompts new questions:

- Why does it work?
- Can it be complete?
- Where will it fail?

The standard model itself hints that the frontier of our ignorance lies at ~ 1 TeV for collisions among the fundamental constituents. In more general terms, the success of our theoretical framework suggests that a significant step beyond present-day energies is needed, to see breakdowns of the theory.

Beyond these generalities, there are many specific issues to be faced. There is, for example, our incomplete understanding of electroweak symmetry breaking and the suggestion (from the "bound" $M_{\rm Higgs} < 1$ TeV/c^2, for example) that the 1 TeV scale will be crucial to a resolution of this problem. The Higgs mechanism provides a means for generating quark and lepton masses and mixing angles, but leaves the values as free parameters. We do not understand what *CP*-violation means. The idea of quark-lepton generations is suggested by the necessity for anomaly cancellation in the electroweak theory, but the *meaning* of generations is unclear. We may even dare to ask what is the origin of the gauge symmetries themselves. Such questions – and this is but a partial list – are stimulated by the standard model itself, and by our desire to find ever simpler descriptions of Nature, of ever more general applicability.

Beyond our search for more complete understanding, there are many reasons to be dissatisfied with the standard model. A powerful aesthetic objection is raised by the arbitrariness of the theory, which requires us to specify a multitude of apparently free parameters:

- 3 coupling parameters α_s, α_{EM}, and $\sin^2\theta_W$,
- 6 quark masses,
- 3 generalized Cabibbo angles,
- 1 *CP*-violating phase,
- 2 parameters of the Higgs potential,
- 3 charged lepton masses,
- 1 vacuum phase angle,

for a total of 19 arbitrary parameters. A similar count holds for the known examples of unified theories of the strong, weak, and electromagnetic interactions, such as $SU(5)$.

At the same time, although the number of fundamental constituents, the quarks and leptons, is small, perhaps it is not small enough. If we count the fundamental fields of the standard model, we find

- 15 quarks (five identified flavors in three colors),
- 6 leptons,
- 1 photon,
- 3 intermediate bosons W^+, W^-, Z^0,
- 8 colored gluons,
- 1 Higgs scalar, and for good measure,
- 1 graviton,

for a total of 35. At least in numerical terms, one may question whether we have advanced very far from the ancient notions of earth, air, fire, and water, interacting by means of love and strife. The thought that there may be too many elementary particles, and a sense of tradition, has led some physicists[3] to suggest that the quarks and leptons – and even the gauge bosons – might themselves be composite.

1.2 Reaching the 1 TeV scale

In the course of these lectures, we shall develop a number of arguments in support of the notion that 1 TeV collisions among the constituents are an important landmark. In Lecture 3, we shall review the unitarity arguments for the scattering of gauge bosons at high energies. In Lecture 4, we shall consider the Higgs particle as a fermion-antifermion composite, as suggested by the Technicolor theories of dynamical symmetry breaking. In Lecture 5, we shall investigate supersymmetry, the fermion-boson symmetry relating particles with spins 0, $\frac{1}{2}$, and 1. Both general arguments and specific inventions for improving the standard model all point to

new phenomena and important clues at energies of ~ 0.3-3 TeV. The accelerators now operating or soon to come into operation will thoroughly explore the few hundred GeV regime. The properties of these machines are summarized in Table 1.

Table 1: Accelerator projects under way

Date	Collisions	Location	$\sqrt{s}$ (TeV)	Mass scale (TeV/c^2)
now	$\bar{p}p$	CERN $S\bar{p}pS$	0.63	~ 0.15
1986	$\bar{p}p$	Fermilab Tevatron	2	~ 0.4
1987	e^+e^-	Stanford SLC	0.1	0.1
1989	e^+e^-	CERN LEP	~ 0.2	~ 0.2
1990	ep	DESY HERA	~ 0.3	~ 0.1

To proceed to the 1 TeV scale with useful luminosity, we may contemplate two possibilities:

- An e^+e^- collider with 1 to 3 TeV per beam;
- A $p^{\pm}p$ collider with 10 to 20 TeV per beam.

With current technology, we know how to build a practical hadron supercollider. An electron-positron collider to explore the 1 TeV scale awaits tests of the linear collider concept at the SLC, and the development of efficient, high-gradient acceleration methods. According to the experts, a serious proposal for such a machine is a decade away.

In this context, a number of machines are under discussion for construction or operation in the mid-1990s:

- SSC: the Superconducting Super Collider in the United States, characterized as a 40 TeV proton-proton machine with an instantaneous luminosity of 10^{33} cm^{-2}sec^{-1}. A conceptual design has recently been submitted to the Department of Energy.

- **LHC: a Large Hadron Collider in the LEP tunnel could be a 10 to 18 TeV $p^{\pm}p$ device with luminosity in the range of $10^{31-33}\text{cm}^{-2}\text{sec}^{-1}$, depending on the approach taken. The high energy option requires the development of 10 Tesla magnets, which has obvious appeal for the future.**

- **CLIC: CERN is also discussing the option of CERN LInear Colliders, now conceived as an e^+e^- facility with $\sqrt{s} = 2$ TeV and $\mathcal{L} = 10^{34}\text{cm}^{-2}\text{sec}^{-1}$.**

There is no doubt that the successful demonstration of linear collider principles at SLC will be followed, after appropriate further development, by an Après-SLC proposal.

A supercollider is a large undertaking. The familiar connection between radius of curvature, momentum, and magnetic field is, in the engineering units appropriate to this application,

$$R = \frac{10}{3}\ \text{km} \cdot \frac{p}{1\ \text{TeV}/c} \cdot \frac{1\ \text{Tesla}}{B}, \tag{1.1}$$

so a circular machine with 20 TeV per beam and 5-Tesla magnets would have a radius of about 13 km. The *SSC* Conceptual Design calls for a tunnel 83 km in circumference. The cost of the *SSC* is estimated at about $\$3 \cdot 10^9$, in 1986 dollars.

1.3 SOME OBJECTIVES OF THESE LECTURES

The goals of our study of supercollider physics were to set out the conventional physics possibilities in some detail, to determine the discovery reach of supercolliders, and to identify areas in which more work is needed. My hopes for this series of lectures will be similar, and I will try to call attention to those areas in which significant new work has been done since the publication of *EHLQ*. The conventional possibilities are important because they are of interest in their own right, and because they provide backgrounds to new or unexpected physics. In assessing what can be explored with a new machine, we considered as examples several of the conventional exotic possibilities: technicolor, supersymmetry, and compositeness. Our calculations are a starting point for considering questions of collider energy and luminosity, and the relative merits of pp and $\bar{p}p$ collisions.

We hope they will also serve as a starting point for the design of detectors and experiments.

Our paper includes treatments of parton distributions, hadron jet production, the standard electroweak theory and minimal extensions to it, technicolor, supersymmetry, and compositeness, We have not dealt with fixed-target physics, log s physics, or exotic states of matter such as QCD plasmas, nor have we carried out detailed Monte Carlo calculations. The reason for the emphasis on hard scattering phenomena is that these include the rare processes which make the most severe demands on machine performance. One look at "soft physics" is revealing, however. At *SSC* energies, we expect the proton-proton total cross section to lie between 100 and 200 mb, as shown in Fig. 2. If the instantaneous luminosity $\mathcal{L} = 10^{33}\text{cm}^{-2}\text{sec}^{-1}$, an *SSC* detector will be confronted with 10^8 interactions per second, a formidable rate.

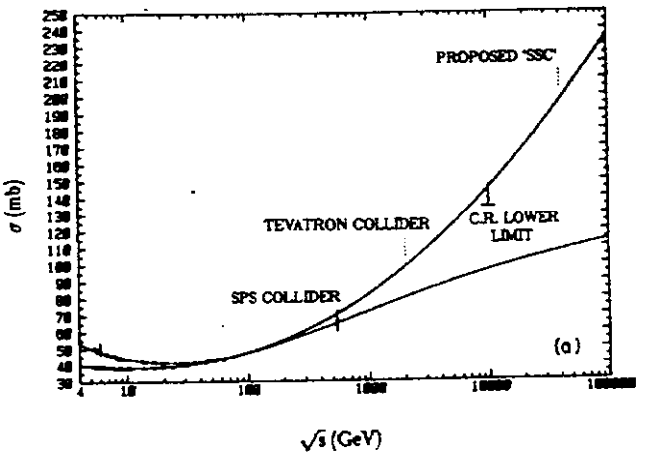

Figure 2: Two extrapolations of the $p^{\pm}p$ total cross sections to supercollider energies [from Ref. 4].

1.4 PARTON DISTRIBUTION FUNCTIONS

The discovery reach of a hadron supercollider is determined by hard scattering processes in which the constituents interact at high energies, as depicted in Fig. 3. Cross sections may be calculated in the renormalization group improved parton model, provided we know the behavior of the quark and gluon distributions within

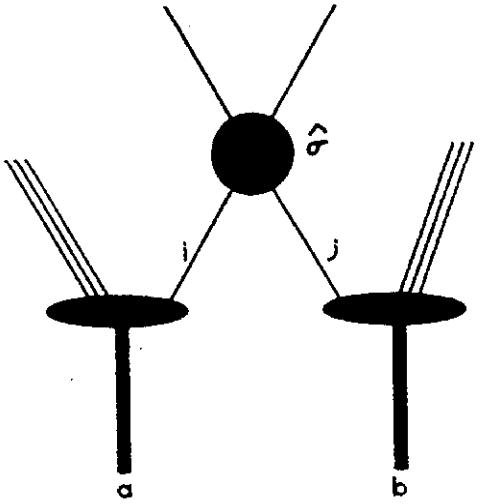

Figure 3: Parton-model representation of a hard-scattering event.

the proton as functions of x and Q^2. For the parton subprocesses of interest, the range over which the structure functions must be known is

$$(10\ \text{GeV})^2 \lesssim Q^2 \lesssim (10^4\ \text{GeV})^2, \tag{1.2}$$

which may correspond to $\langle x \rangle$ as small as 10^{-4}. With the parton distributions written as $f_i^{(a)}(x, Q^2)$ for the number density of partons of species i in hadron a, hadronic cross sections are given schematically by

$$\begin{aligned} d\sigma(a+b \to c+X) \;&=\; \sum_{ij} \int dx_a dx_b \cdot \\ &\qquad f_i^{(a)}(x_a, Q^2) f_j^{(b)}(x_b, Q^2) d\hat{\sigma}(i+j \to c+X), \end{aligned} \tag{1.3}$$

where $d\hat{\sigma}$ represents the elementary cross section. The parton-level cross sections are known for a great many reactions of potential interest.

Some care is required in devising structure functions for application to supercollider physics. The pre-existing parametrizations given in the literature are valid only over limited ranges of Q^2 which are much smaller than the range given by (1.2). In addition, structure functions are essentially unmeasured in deeply inelastic scattering experiments for $x \lesssim 0.01$, so it is important to consider the reliability of extrapolations to small values of x and large values of Q^2. A comprehensive discussion is given in *EHLQ*. A quick summary of the basic ideas will better serve our purposes here.

Probing a quark inside a proton with a virtual photon characterized by Q^2 is sensitive to fluctuations on a scale characterized by $1/Q^2$. For a short interval, the quark may fluctuate into a quark plus a gluon. We may write the probability to observe a quark carrying a fraction z of the parent quark's momentum as

$$\frac{\alpha_s(Q^2)}{\pi} P_{q\leftarrow q}(z) \cdot d\log Q^2, \tag{1.4}$$

where $P_{q\leftarrow q}(z)$ is the Altarelli-Parisi[5] "splitting function," calculable in QCD perturbation theory. Using the shorthand $\tau \equiv \log Q^2$, we may write the evolution of the quark distribution function as

$$\frac{dq(x,\tau)}{d\tau} = \frac{\alpha_s(\tau)}{\pi} \int_x^1 \frac{dy}{y} q(y,\tau) P_{q\leftarrow q}(z,\tau), \tag{1.5}$$

with $x = zy$. Any quark observed with a momentum fraction x of the proton necessarily had a parent with momentum fraction $y \geq x$.

It is convenient to parametrize parton distributions in terms of

$$\begin{aligned} \text{up quarks} &: u_v(x,Q^2) + u_s(x,Q^2) \\ \text{down quarks} &: d_v(x,Q^2) + d_s(x,Q^2) \\ \text{up antiquarks} &: u_s(x,Q^2) \\ \text{down antiquarks} &: d_s(x,Q^2) \\ \text{heavy quarks and antiquarks} &: q_s(x,Q^2) \\ \text{gluons} &: G(x,Q^2). \end{aligned} \tag{1.6}$$

The valence (or "nonsinglet") distributions satisfy the evolution equation

$$\begin{aligned} \frac{dp(x,Q^2)}{d\log Q^2} &= \frac{2\alpha_s(Q^2)}{3\pi} \int_x^1 dz \frac{(1+z^2)p(y,Q^2) - 2p(x,Q^2)}{1-z} \\ &\quad + \frac{\alpha_s(Q^2)}{\pi} \left[1 + \frac{4\log(1-x)}{3}\right] p(x,Q^2), \end{aligned} \tag{1.7}$$

where $p = xu_v$ or xd_v and $y = x/z$. The evolution of the valence quarks thus depends upon the valence quark distributions alone.

In contrast, sea quarks can emerge from the fluctuation of parent sea quarks, or from the splitting of parent gluons into quark antiquark pairs. Thus the evolution of sea quark distributions depends explicitly on the distributions of sea quarks and gluons. Gluons may be generated in the fluctuation of valence or sea quarks, and

in the splitting of parent gluons into two gluons. Their evolution is thus dependent upon the input distributions of valence quarks, sea quarks, and gluons.

The input distributions are determined from experiments on deeply inelastic scattering of leptons from nucleon targets. For example, the valence quark distribution is measured directly as

$$x\left[u_v(x,Q^2)+d_v(x,Q^2)\right] = \frac{\pi}{G_F^2 ME}\cdot\frac{1}{1-(1-y)^2} \cdot\left[\frac{d\sigma(\nu N\to\mu^- X)}{dxdy}-\frac{d\sigma(\bar{\nu}N\to\mu^+ X)}{dxdy}\right], \tag{1.8}$$

where $x = Q^2/2M\nu$, $y = \nu/E$, $\nu = E - E_\mu$, and $N \equiv \frac{1}{2}(p+n)$ is an "isoscalar nucleon." The distributions of valence up and down quarks may be separated by making separate measurements on hydrogen and deuterium targets. The up and down sea distributions are determined from measurements of $\mathcal{F}_2$ under the assumption that $u_s = d_s$, and the strange sea may be determined from the reaction

$$\begin{array}{rcl} \bar{\nu}\,\bar{s} & \to & \mu^+\bar{c}+X \\ & & \hookrightarrow \mu^- + \cdots \end{array} \tag{1.9}$$

The shape of the gluon distribution cannot be measured directly in electroweak interactions. The first moment, $\int_0^1 dx x G(x,Q^2)$, can be determined from the momentum sum rule. The shape of $G(x,Q^2)$ is strongly correlated with the strong coupling constant α_s, or equivalently with the QCD scale parameter Λ. A large value of Λ implies rapid evolution, and so requires a broad initial distribution. A small value of Λ implies a slower evolution, which corresponds to a narrower initial distribution. Ideally, one would like to determine Λ precisely from the evolution of the valence distribution, and then extract the gluon distribution $G(x,Q^2)$ from the evolution of the flavor-singlet (sea) distribution functions. Limited statistics have prevented this possibility until now.

In *EHLQ* we produced two sets of distribution functions that behave sensibly over the kinematic range of interest. This was done by constructing initial distributions at $Q_0^2 = 5$ GeV^2 using the CDHS structure functions,[6] subject to the constraints of momentum and flavor sum rules, and under the assumption that there are no "intrinsic" heavy flavor components. We then evolved the distributions to $Q^2 > Q_0^2$ using the (first-order) Altarelli-Parisi equations. We studied in

detail two distributions, characterized by the QCD scale parameters $\Lambda = 200$ MeV and 290 MeV, and gave a detailed discussion of the uncertainties.

The uncertainties fall into several classes. The first has to do with uncertainties in the input. We studied with some care the effect of our ignorance at small x and small Q^2, and found that at moderate to large values of Q^2 the small-x structure functions could be computed without great ambiguity. The size of the input sea distribution is subject to question, both because of other measurements,[7] and the EMC effect.[8] The ratio of down to up quarks in our parametrizations do not perfectly reproduce the SLAC-MIT measurements,[9] but are in acceptable agreement with the EMC data.[10] At the factor-of-two level of reliability for which one hopes in making supercollider projections, none of this matters. It is still desirable, particularly for $S\bar{p}pS$ and Tevatron applications, to do better. We expect that final data from the CDHS and CCFR neutrino experiments will soon be available, and we intend to make use of these to produce revised distributions. In the longer term, results from the fixed-target Tevatron experiments should be helpful. We may also ask whether collider determinations of structure functions can become quantitative, instead of merely (already very interesting) consistency checks.

A second area of uncertainty surrounds the treatment of heavy flavors. The *EHLQ* distributions include only the perturbative evolution of heavy quark components. The treatment of thresholds is somewhat uncertain. More complete data on $\mu N \to \mu c\bar{c}X$ (perhaps ultimately $\mu N \to \mu b\bar{b}X$) will eventually provide useful guidance. In addition, some programming errors led to an underestimate of the heavy-quark population in the original *EHLQ* structure functions. Better treatments have recently been given by Collins and Tung[11], and by us.[12] None of these treatments includes any contribution of "intrinsic" heavy flavors. The experimental situation for charm is so confused[13] that one is free to believe almost anything. However, there is now general agreement[14] that this component would scale as $1/m^4_{quark}$, and so be completely irrelevant for flavors heavier than charm. We may note here that the existence of light squarks or gluinos would make a (small) difference in the evolution of structure functions.

A final uncertainty concerns a question of principle: does QCD perturbation theory, as embodied in the Altarelli-Parisi equations, make sense as $x \to 0$? The

concern here is that the pileup of $\log x$ factors might make the perturbation series meaningless for x very close to zero. How close? Gribov, Levin, and Ryskin[15] have given a careful, and very physical, analysis of this problem, which has recently been extended by Mueller and Qiu.[16] They argue that if the quantity

$$D(x,Q^2) = \frac{x f_i(x,Q^2) m_\pi^2}{Q^2} \gtrsim 1, \tag{1.10}$$

partons overlap and cease to act individually so that conventional "free-parton" perturbation theory cannot be trusted. It was shown at Snowmass '84[17] that the *EHLQ* structure functions evade the dangerous regime for all values of $x > 10^{-4}$ and for 5 GeV^2 $< Q^2 <$ 10^8 GeV^2, the range in which it was hoped to apply them.

The general conclusion is that we know enough to make reasonably reliable projections to supercollider energies. Our knowledge of the parton distributions is well matched to our knowledge of the elementary cross sections, and to our current needs. Refinements seem both interesting and possible.

LECTURE 2: QCD PHYSICS

The observation[18] of hadron jets in e^+e^- annihilations provided an early confirmation of the pointlike nature of quarks and the utility of the quark-parton model for dynamics. The suggestion[19] that the lowest order two parton to two parton process (the QCD analog of Bhabha scattering) should lead to two-jet final states in hadron-hadron collisions was only verified with great clarity with the coming of the initial data from the $S\bar{p}pS$ collider at CERN.[20] We now have reason to hope that the scattering mechanism can be studied in detail, and that multijet spectroscopy will emerge as a powerful experimental tool.

2.1 TWO-JET EVENTS

If partons i and j with incident momenta p_1 and p_2 initiate a two-body collision with outgoing momenta p_3 and p_4, it is useful to employ the parton-level

Mandelstam invariants

$$\left.\begin{aligned} \hat{s} &= (p_1+p_2)^2 \\ \hat{t} &= (p_1-p_3)^2 \to -(\hat{s}/2)(1-\cos\theta^*) \\ \hat{u} &= (p_1-p_4)^2 \to -(\hat{s}/2)(1+\cos\theta^*) \end{aligned}\right\}. \tag{2.1}$$

The elementary cross section $\hat{\sigma}(\hat{s},\hat{t},\hat{u}) \sim O(\alpha_s^2)$ will lead to two-jet final states when $\hat{s}$ and $\hat{t}$ are "large."

In the hadronic collision itself, useful kinematic variables are the jet rapidities

$$y_i = \frac{1}{2}\log\frac{E+p_\parallel}{E-p_\parallel} \tag{2.2}$$

and $p_\perp$, the transverse momentum of either jet. The cross section for the production of two jets in the collision of hadrons a and b is then represented as

$$\frac{d^3\sigma}{dy_1 dy_2 dp_\perp} = \frac{2\pi\tau p_\perp}{\hat{s}}\sum_{ij}\frac{1}{1+\delta_{ij}} f_i^{(a)}(x_a,M^2) f_j^{(b)}(x_b,M^2)\hat{\sigma}_{ij}(\hat{s},\hat{t},\hat{u}). \tag{2.3}$$

An immediate ambiguity arises in the lowest-order calculation: what value is to be taken for the scale M^2? Although a full evaluation[21] of the $O(\alpha_s^3)$ corrections shows that there is no simple answer, the choice $M^2 = p_\perp^2/4$ has sometimes been suggested as minimizing higher-order effects.

The Born diagrams for two-body scattering in QCD are shown in Fig. 4. If we idealize the partons as massless, we may write the $2 \to 2$ parton cross sections as

$$\frac{d\hat{\sigma}}{d\hat{t}} = \frac{\pi\alpha_s(Q^2)^2}{\hat{s}^2}|\mathcal{M}|^2, \tag{2.4}$$

where $|\mathcal{M}|^2$, the dimensionless square of the matrix element, is averaged over initial colors and spins, and summed over final colors and spins. Expressions for the matrix elements[22] are collected in Table 2. The angular distributions corresponding to these elementary processes are sketched in Fig. 5. The dominant characteristic of many of these reactions is an angular dependence

$$\frac{d\sigma}{d\cos\theta^*} \sim \frac{1}{(1-\cos\theta^*)^2}, \tag{2.5}$$

arising from the t-channel gluon exchange, analogous to the t-channel photon exchange that drives the Rutherford formula. In terms of the variable $\chi \equiv \cot^2(\theta^*/2)$, the angular distribution may be reëxpressed as

$$\frac{d\sigma}{d\chi} \sim \text{constant}. \tag{2.6}$$

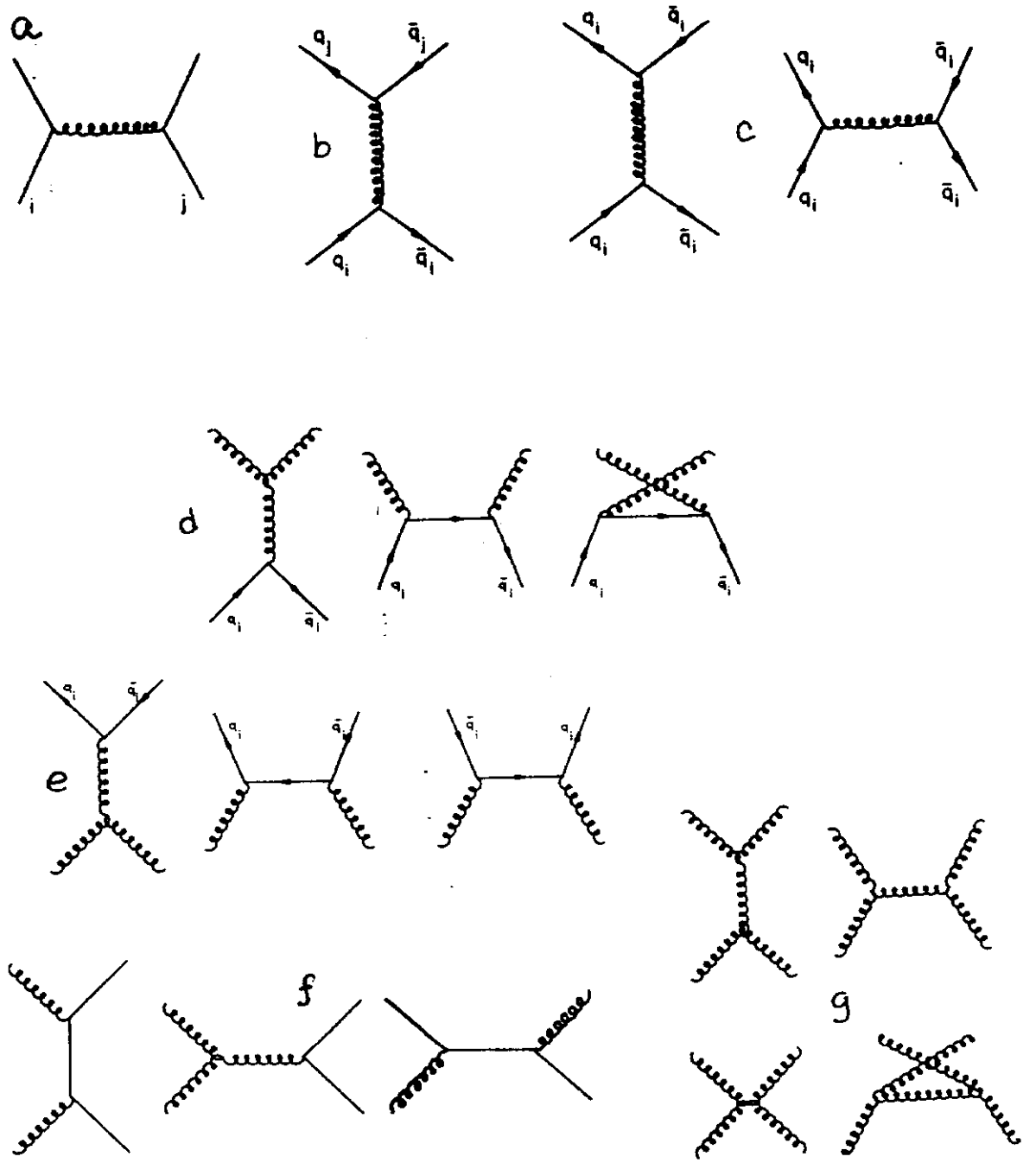

Figure 4: $O(\alpha_s^2)$ contributions to parton-parton scattering in QCD. (a) $q_i q_j \to q_i q_j$ or $q_i \bar{q}_j \to q_i \bar{q}_j, i \neq j$. (b) $q_i \bar{q}_i \to q_j \bar{q}_j, i \neq j$. (c) $q_i \bar{q}_i \to q_i \bar{q}_i$. (d) $q_i \bar{q}_i \to gg$. (e) $gg \to q_i \bar{q}_i$. (f) $gq \to gq$ or $g\bar{q} \to g\bar{q}$. (g) $gg \to gg$.

Table 2: Feynman amplitudes for parton-parton scattering, in QCD.

Process	$\lvert\mathcal{M}\rvert^2$	value at $\theta^* = \pi/2$
$q_i q_j \to q_i q_j$	$\frac{4}{9} \cdot \frac{\hat{s}^2 + \hat{u}^2}{\hat{t}^2}$	2.22
$q_i q_i \to q_i q_i$	$\frac{4}{9}\left(\frac{\hat{s}^2 + \hat{u}^2}{\hat{t}^2} + \frac{\hat{s}^2 + \hat{t}^2}{\hat{u}^2}\right) - \frac{8}{27} \cdot \frac{\hat{s}^2}{\hat{t}\hat{u}}$	3.26
$q_i \overline{q}_i \to q_j \overline{q}_j$	$\frac{4}{9} \cdot \frac{\hat{t}^2 + \hat{u}^2}{\hat{s}^2}$	0.22
$q_i \overline{q}_i \to q_i \overline{q}_i$	$\frac{4}{9}\left(\frac{\hat{s}^2 + \hat{u}^2}{\hat{t}^2} + \frac{\hat{u}^2 + \hat{t}^2}{\hat{s}^2}\right) - \frac{8}{27} \cdot \frac{\hat{u}^2}{\hat{t}\hat{s}}$	2.59
$q_i \overline{q}_i \to g g$	$\frac{32}{27} \cdot \frac{\hat{u}^2 + \hat{t}^2}{\hat{u}\hat{t}} - \frac{8}{3} \cdot \frac{\hat{u}^2 + \hat{t}^2}{\hat{s}^2}$	1.04
$g g \to q_i \overline{q}_i$	$\frac{1}{6} \cdot \frac{\hat{u}^2 + \hat{t}^2}{\hat{u}\hat{t}} - \frac{3}{8} \cdot \frac{\hat{u}^2 + \hat{t}^2}{\hat{s}^2}$	0.15
$g q_i \to g q_i$	$-\frac{4}{9} \cdot \frac{\hat{u}^2 + \hat{s}^2}{\hat{u}\hat{s}} + \frac{\hat{u}^2 + \hat{s}^2}{\hat{t}^2}$	6.11
$g g \to g g$	$\frac{9}{2}\left(3 - \frac{\hat{u}\hat{t}}{\hat{s}^2} - \frac{\hat{u}\hat{s}}{\hat{t}^2} - \frac{\hat{s}\hat{t}}{\hat{u}^2}\right)$	30.4

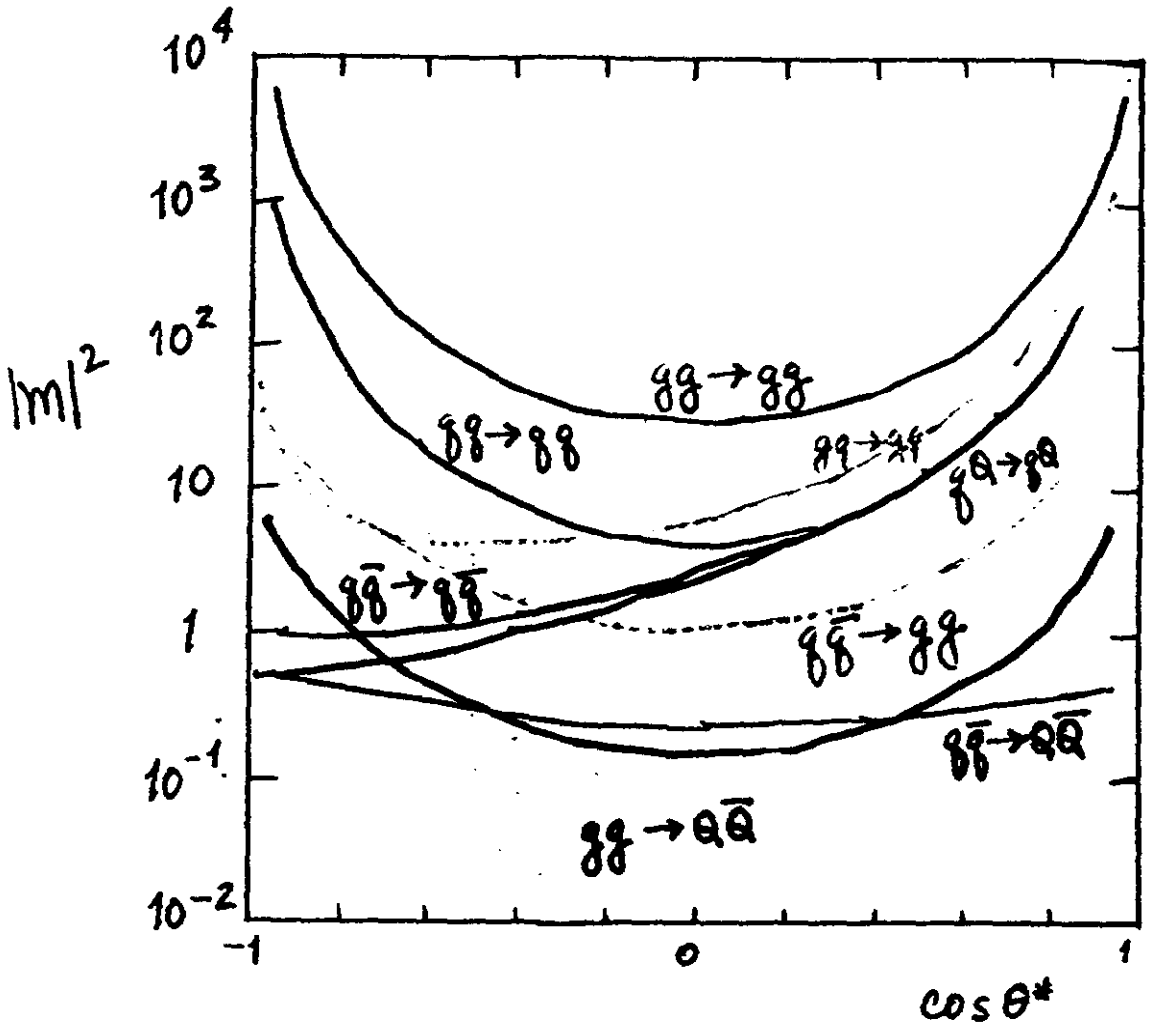

Figure 5: Angular distributions given by the Born terms for parton-parton scattering in QCD (after Ref. 23).

I show in Fig. 6 the angular distribution of two-jet events in the dijet c.m. frame, for dijets with effective masses in the interval

$$150 \text{ GeV}/c^2 < M(jet - jet) < 250 \text{ GeV}/c^2, \tag{2.7}$$

as observed by the UA-1 Collaboration.[24] To first approximation, the distribution is flat as our simple analogy with Rutherford scattering would suggest. In more detail, it agrees very precisely with the prediction of the parton model, shown as the solid curve.

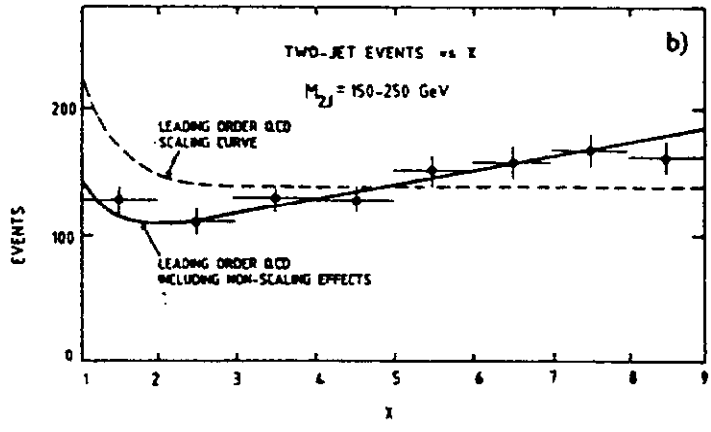

Figure 6: Angular distribution of two jet events observed by the UA-1 Collaboration in $\bar{p}p$ collisions at $\sqrt{s} = 540$ GeV, as described in the text. The curve shows the shape predicted by the QCD Born terms convoluted with the *EHLQ* structure functions (Set 1).

A further indication that the parton-model procedure is sound, and that knowledge of the structure functions derived from experiments on deeply inelastic lepton scattering is adequate, is provided by other $S\bar{p}pS$ data on hadron jets. Figure 7 shows representative data from the UA-1 Collaboration[25] on the inclusive jet cross section $d\sigma/dp_\perp dy\,|_{y=0}$, compared with the predictions of the QCD Born term. The agreement is quite satisfactory.[26]

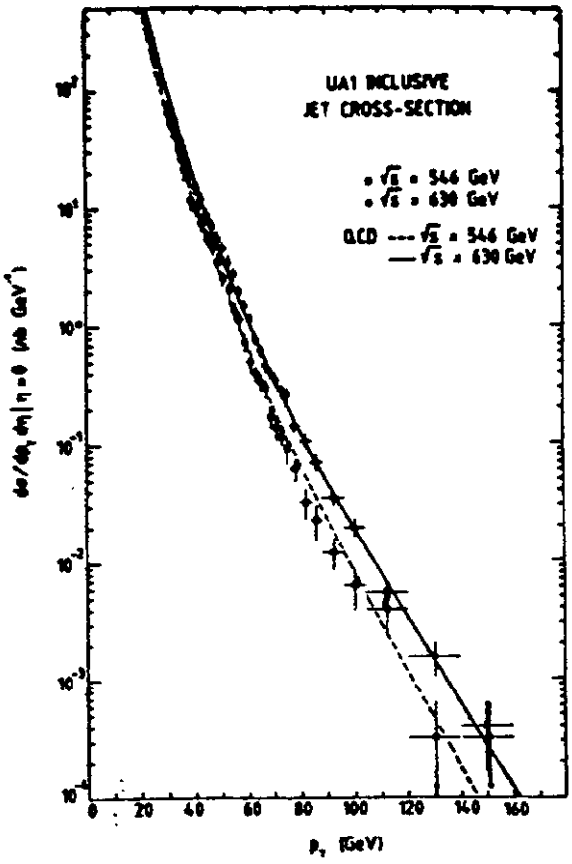

Figure 7: The inclusive jet cross section for the pseudorapidity interval $|\eta| < 0.7$, as a function of the jet transverse momentum, as measured by the UA-1 Collaboration. The open dots correspond to the data at $\sqrt{s} = 546$ GeV and the solid dots to those at $\sqrt{s} = 630$ GeV.

Thus satisfied with the reasonableness of our procedure, we may make the extrapolation to supercollider energies. A useful way to display the results is to examine the trigger rate for events with transverse energy E_T greater than some threshold E_T^{min}. This is shown in Fig. 8 for the nominal operating conditions of the *SSC*: $\sqrt{s} = 40$ TeV and $\mathcal{L} = 10^{33}$ cm^{-2}sec^{-1}, as well as at 10 and 100 TeV. At 40 TeV, a "high-E_T" trigger with threshold set at 2 TeV will count at 1 Hz from two-jet QCD events. This is of interest in planning triggers which will efficiently select "interesting" events from the $2 \cdot 10^8$ interactions which will take place each second in an *SSC* interaction region.

We can show in perturbative QCD that jets should exist, and become increasingly collimated with increasing jet energies. If $\delta(E)$ defines an angular cone

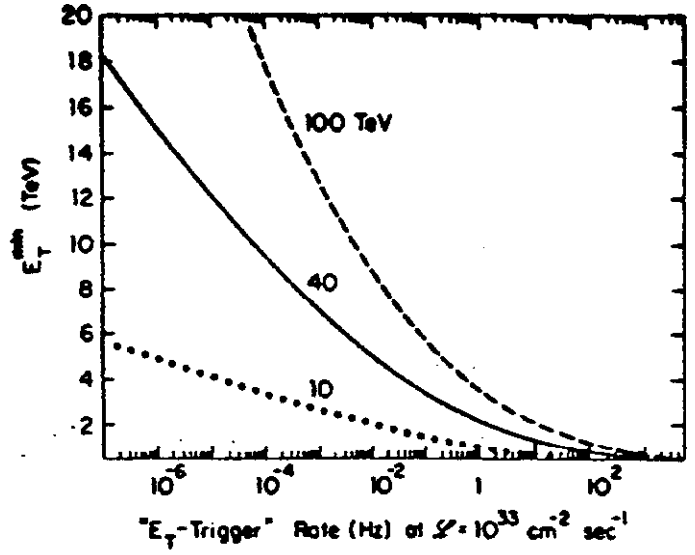

Figure 8: Counting rate for an E_T-trigger in pp collisions at an instantaneous luminosity of $\mathcal{L} = 10^{33}$ cm^{-2}sec^{-1} (after *EHLQ*). The threshold is defined for transverse energy deposited in the central region of rapidity, defined by $|y_i| < 2.5$ for jets 1 and 2.

containing some fixed fraction of the jet energy, then[27]

$$\delta(E) \sim E^{-1/4}. \tag{2.8}$$

Gluon jets should be broader than quark jets.[28] For the same fractional energy contained in a cone,

$$\delta_{gluon} = [\delta_{quark}]^{4/9}. \tag{2.9}$$

2.2 SOURCES OF HEAVY QUARKS

The sources of heavy quarks are strong-interaction production in the reactions $gg \to Q\overline{Q}$ and $q\overline{q} \to Q\overline{Q}$, and electroweak production through the decays of $W^{\pm}$ and Z^0. The latter have the advantage of known cross sections, which is to say cross sections that can be measured from the leptonic decays of the gauge bosons, and calculable branching ratios. Howevever, they lead to very large rates only for the decays of real (not virtual) gauge bosons. This makes them an attractive option for the top-quark search at the $S\overline{p}pS$ and at the Tevatron.

The cross sections for the strong interaction processes are known in QCD perturbation theory:[29]

$$\frac{d\hat{\sigma}(gg \to Q\overline{Q})}{d\hat{t}} = \frac{\pi\alpha_s^2}{8\hat{s}^2}\cdot\left\{\frac{6(\hat{t}-m^2)(\hat{u}-m^2)}{\hat{s}^2}+\right. \tag{2.10}$$
$$\left[\left(\frac{4}{3}\cdot\frac{(\hat{t}-m^2)(\hat{u}-m^2)-2m^2(\hat{t}+m^2)}{(\hat{t}-m^2)^2}\right.\right.$$
$$\left.+\frac{3(\hat{t}-m^2)(\hat{u}-m^2)+m^2(\hat{u}-\hat{t})}{\hat{s}(\hat{t}-m^2)}\right)$$
$$\left.\left.+\ (t\leftrightarrow u)\right]-\frac{m^2(\hat{s}-4m^2)}{3(\hat{t}-m^2)(\hat{u}-m^2)}\right\},$$

which is generally dominant, and

$$\frac{d\hat{\sigma}(q\overline{q} \to Q\overline{Q})}{d\hat{t}} = \frac{4\pi\alpha_s^2}{9\hat{s}^2}\left[\frac{(\hat{t}-m^2)^2+(\hat{u}-m^2)^2+2m^2\hat{s}}{\hat{s}^2}\right], \tag{2.11}$$

which is generally negligible.

I show in Fig. 9 the yield of heavy quarks from these sources for the $\overline{p}p$ colliders. Similar results are given for supercollider energies in *EHLQ*. A word of caution is in order for these estimates. When the "heavy" quark is light on the scale set by the elementary collisions, the next-order production process $gg \to Q\overline{Q}$ may

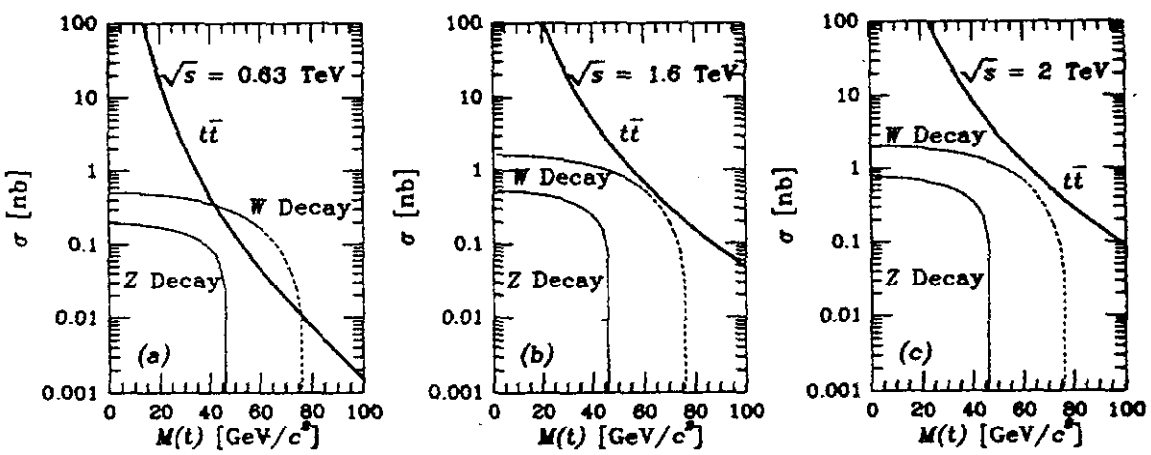

Figure 9: Cross sections for the production of t or $\bar{t}$ quarks in $\overline{p}p$ collisions as a function of the mass of the heavy quark. (a) $\sqrt{s} = 630$ GeV; (b) $\sqrt{s} = 1600$ GeV; (c) $\sqrt{s} = 2000$ GeV.

dominate.[30] A simple estimate will show why this is so. For $s_{Q\overline{Q}}/\hat{s} \ll 1$ and $\hat{s} \gg 4M_Q^2$, we may approximate the cross section by considering the process

$$\begin{array}{ccc} gg & \rightarrow & gg \\ & & \hookrightarrow Q\overline{Q}, \end{array} \tag{2.12}$$

the branching of a produced gluon into a $Q\overline{Q}$ pair. The ratio of three-body and two-body cross sections will be

$$\begin{aligned} \frac{\sigma(gg \rightarrow gQ\overline{Q})}{\sigma(gg \rightarrow Q\overline{Q})} &\simeq \underbrace{\frac{\sigma(gg \rightarrow gg)}{\sigma(gg \rightarrow Q\overline{Q})}}_{O(100)} \cdot \underbrace{\frac{\alpha_s}{3\pi}}_{0.02} \cdot \underbrace{\log\left(\frac{\hat{s}}{4M_Q^2}\right)}_{2-4} \\ &\simeq O(5-10), \end{aligned} \tag{2.13}$$

where we have taken the ratio of the two-body cross sections from Table 2.

The three-body reaction mechanism is undoubtedly already preeminent for b-quark production at the $S\overline{p}pS$. The two mechanisms may of course readily be distinguished topologically. The $Q\overline{Q}$ final state leads to heavy quarks on opposite sides of the beam axis, whereas the $gQ\overline{Q}$ final state places both heavy quarks on the same side of the beam axis.

2.3 Multijet Final States

Multiparton final states are important. Two-, three-, and four- (and more) jet final states have an inherent interest in QCD, and must be understood as potential backgrounds to new physics. The W+jet, W+two jets ...final states may constitute precision tests of QCD, and are important sources of "jet plus missing energy" events.

Experimental work at the $S\overline{p}pS$ collider and considerations of new-physics signals at the SSC make progress in understanding these multiparton final states extremely desirable. However, the calculations of many-parton amplitudes are challenging. For example, the computation of the $gg \rightarrow gggg$ amplitudes is impossible (you may take this as a definition) by conventional methods. Over the past two years, new and more efficient techniques have been developed, refined, and applied to these problems. The new methods have two essential features:

- **Calculate *helicity amplitudes* rather than matrix elements squared;**

- **Simplify the calculation of helicity amplitudes:**

  (i) **Exploit the gauge invariance of the theory and the masslessness of particles; *OR***

  (ii) **Relate the desired amplitude to easily calculated amplitudes in a simpler theory by supersymmetry.**

These rules follow from the observation that amplitudes involving vector particles give rise to many terms at intermediate stages of the calculations, most of which cancel in the final result. There are great advantages in trying to gain control over the spurious terms.

Two novel methods are now coming into general use. The first is the so-called "CALKUL" method,[31] which is well suited to the problem of radiation from zero-mass fermion lines. It is based on the idea that a particular gauge choice may simplify the evaluation of tree diagrams. As an example, let us consider the reaction

$$e^+(p_+)e^-(p_-) \to \gamma(k_1)\gamma(k_2), \tag{2.14}$$

which is represented in lowest order by the familiar t- and u-channel diagrams. An essential aspect of the "CALKUL" procedure is to express polarization vectors in terms of vectors already present in the problem. To see why this may be useful, consider one of the terms in the amplitude for reaction (2.14),

$$\mathcal{M} \sim \bar{v}(p_+)\not{\epsilon}_1 \boxed{\frac{(\not{p}_- - \not{k}_2)}{(p_- - k_2)^2}\not{\epsilon}_2 u(p_-)}. \tag{2.15}$$

If we express the polarization four-vector as

$$\not{\epsilon}_i^{(\pm)}(k_i) = N\left[\not{k}_i\not{p}_+\not{p}_-(1 \pm \gamma_5) - \not{p}_+\not{p}_-\not{k}_i(1 \mp \gamma_5)\right], \tag{2.16}$$

then only one term contributes, because

$$\not{p}_- u(p_-) = 0 = \bar{v}(p_+)\not{p}_+. \tag{2.17}$$

The remaining term cancels the denominator of the fermion propagator, so the boxed piece of the equation gives simply

$$(\not{p}_- - \not{k}_2)p_+(1 \mp \gamma_5)u(p_-), \tag{2.18}$$

for $p_i^2 = k_i^2 = 0$, which is a simple form.

The idea of the supersymmetry method is to imagine an extension of QCD which exactly respects $N = 2$ supersymmetry.[32] We are not imagining that this is an approximate symmetry of Nature; it need only be a construct used as a calculational tool. Corresponding to the spin-1 gluon g are the spin-$\frac{1}{2}$ gluino $\tilde{g}$ and the spin-0 scalar gluon ϕ_g. The interactions of all these particles are related by the supersymmetry of the Lagrangian, and as a result, all helicity amplitudes are related.

Perhaps the simplest example, and yet one of great practical importance, is to relate $\mathcal{M}(gg \to gg)$ to $\mathcal{M}(\phi_g\phi_g \to \phi_g\phi_g)$. In this case, there is one single independent helicity amplitude (for the $++ \to ++$ transition, from which all others may be obtained by crossing). For the analog reaction, the external particles are all spinless, so the evaluation of the amplitude is greatly simplified. Using these methods, previously known results for 2-to-2 and 2-to-3 reactions are obtained very simply. New results for 2-to-4 reactions do not require superhuman effort.

During 1985, all the 2-to-4 QCD amplitudes have been evaluated by these new techniques, in a form suitable for fast computation.[33] The remaining challenge, for the moment, is to learn how to turn these cross section expressions into simulations and insights applicable to experiment.

LECTURE 3: ELECTROWEAK PHENOMENA

3.1 GENERALITIES

The standard model is built upon three quark and lepton generations that transform under $SU(2)_L \otimes U(1)_Y$ as

$$\underbrace{\begin{pmatrix} u \\ d_\theta \end{pmatrix}_L}_{\text{lefthanded doublets}} \qquad \underbrace{u_R,\ d_R}_{\text{righthanded singlets}} \qquad \begin{matrix} Y_L = 1/3;\ Y_R = \begin{pmatrix} 4/3 \\ -2/3 \end{pmatrix} \\ \\ \underbrace{\begin{pmatrix} \nu_e \\ e \end{pmatrix}_L} \qquad \underbrace{e_R} \qquad\qquad Y_L = -1;\ Y_R = -2 \end{matrix} \quad , \tag{3.1}$$

where the weak-isospin and hypercharge assignments guarantee that the Gell-Mann–Nishijima formula

$$Q = I_3 + \tfrac{1}{2}Y \tag{3.2}$$

yields the appropriate charges. The gauge bosons of the unbroken theory are

$$\underbrace{W^+, W_3, W^-}_{SU(2)_L} \quad \underbrace{A}_{U(1)_Y} \ . \tag{3.3}$$

To break the gauge symmetry $SU(2)_L \otimes U(1)_Y \to U(1)_{EM}$, we add to the standard gauge theory a complex scalar doublet ϕ with gauge-invariant couplings to itself, to gauge bosons, and to fermions. The construction of the theory is explained in detail in many textbooks.[34]

After the introduction of a Higgs potential

$$V(\phi^\dagger\phi) = \mu_0^2 \phi^\dagger\phi + |\lambda| (\phi^\dagger\phi)^2 \tag{3.4}$$

with $\mu_0^2 < 0$ for the self-interactions of the scalars, the gauge symmetry is spontaneously broken and the scalar field acquires a vacuum expectation value

$$\begin{aligned} \langle\phi\rangle &= \sqrt{-\mu_0^2/2\,|\lambda|} \\ &= (G_F\sqrt{8})^{-1/2} \\ &\simeq 175\ \text{GeV} \ , \end{aligned} \tag{3.5}$$

where the numerical value is fixed by the low-energy phenomenology. The result of the spontaneous symmetry breaking is that the three would-be Goldstone bosons corresponding to the three broken generators of $SU(2)_L \otimes U(1)_Y$ become the longitudinal components of W^+, W^-, and

$$Z = (gW_3 - g'A)/\sqrt{g^2 + g'^2}\,, \tag{3.6}$$

where g and $g'/2$ are the coupling constants of the $SU(2)_L$ and $U(1)_Y$ gauge groups, respectively. The photon, which corresponds to the unbroken generator of the $U(1)_{EM}$ symmetry, remains massless.

In contrast to the definite predictions

$$\left.\begin{aligned} M_W &= g\,\langle\phi\rangle \\ M_Z &= \sqrt{g^2 + g'^2}\,\langle\phi\rangle \end{aligned}\right\} \tag{3.7}$$

for the masses of the intermediate bosons, the mass of the neutral scalar (the "Higgs boson") that remains as a physical particle as a consequence of the spontaneous symmetry breaking is <u>not</u> predicted.

3.2 Issues

The principal standard model issues to be addressed with a multi-TeV hadron collider are these:

- The rate of $W^\pm$ and Z^0 production. This is chiefly of interest for investigations of the production mechanism itself and for the study of rare decays of the intermediate bosons. We expect that by the time a supercollider comes into operation the more basic measurements such as precise determinations of the masses and widths of the intermediate bosons will have been accomplished.

- The cross section for pair production of gauge bosons. These are sensitive to the structure of the trilinear couplings among gauge bosons, and must be understood as potential backgrounds to the observation of heavy Higgs bosons, composite scalars, and other novel phenomena.

- **The Higgs boson itself. In the minimal electroweak model, this is the lone boson remaining to be found. Elucidating the structure of the Higgs sector (and mot merely finding a single Higgs scalar) is one of the primary goals of experimentation in the TeV regime.**

Let us take a moment to look briefly at each of these points.

The integrated cross sections for W^+ and W^- production in pp collisions are shown in Fig. 10 as functions of the c.m. energy $\sqrt{s}$. Also shown are the cross sections for production of $W^\pm$ in the rapidity interval $-1.5 < y < 1.5$. The number of intermediate bosons produced at a high-luminosity supercollider is impressively large. At 40 TeV, for example, a run with an integrated luminosity of 10^{40} cm^{-2} would yield approximately $6 \cdot 10^8$ Z^0s and $2 \cdot 10^9$ $W^\pm$s. For comparison, at a high-luminosity Z^0 factory such as LEP ($\mathcal{L} \simeq 2 \cdot 10^{31}$ cm^{-2}sec^{-1}) the number of Z^0s expected in a year of running is approximately 10^7. There is no competitive source of *charged* intermediate bosons (*cf.* Table 3).

The angular distribution of the produced intermediate bosons is of great importance for the design of experiments. At supercollider energies, many intermediate bosons will be produced within a narrow cone about the beam direction. In a 40 TeV machine with an average luminosity of 10^{33}, there will be a flux of about 10

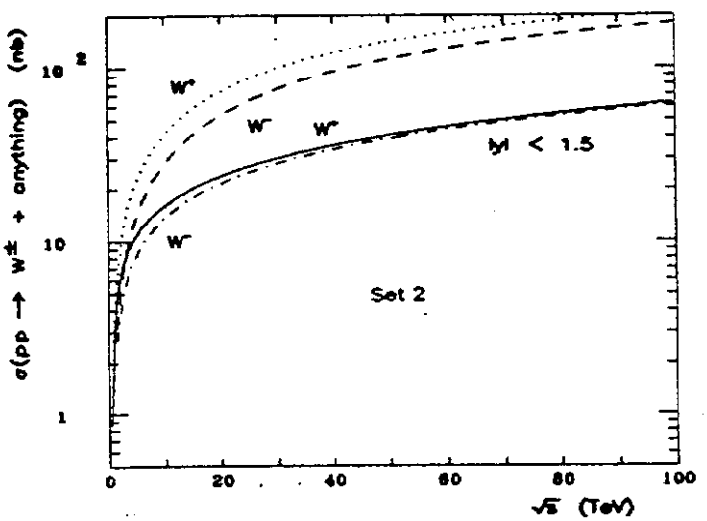

Figure 10: Cross sections for $W^\pm$ production in pp collisions in the Drell-Yan picture, integrated over all rapidities, and restricted to the interval $|y| < 1.5$ (after *EHLQ*).

Table 3: Sources of Intermediate Bosons

Collider	Beams	$\sqrt{s}$	$\mathcal{L}$ [cm^{-2}sec^{-1}]	$W^{\pm}$	Z^0
$S\bar{p}pS$	$\bar{p}p$	630 GeV	10^{30}	4 nb	1.2 nb
				$4 \cdot 10^4$	$1.2 \cdot 10^4$
Tevatron	$\bar{p}p$	1.6 TeV	10^{30}	15 nb	3 nb
				$1.5 \cdot 10^5$	$3 \cdot 10^4$
		2 TeV	10^{31}	17 nb	3.6 nb
				$1.7 \cdot 10^6$	$3.6 \cdot 10^5$
SLC	e^+e^-	93 GeV	10^{31}		46 nb
					$4.6 \cdot 10^6$
LEP	e^+e^-	93 GeV	10^{32}		46 nb
					$4.6 \cdot 10^7$
SSC	pp	40 TeV	10^{33}	220 nb	72 nb
				$2.2 \cdot 10^9$	$7 \cdot 10^8$

W^+/second emitted within 2° of the beam direction, in each hemisphere. Special purpose detectors deployed near the forward direction may thus have significant advantages for the study of rare decays.

The $p_\perp$-distributions of intermediate bosons, and the structure of events containing intermediate bosons and one or more hadron jets can serve as important tests of QCD. Calculations are essentially complete[35] for W + jet, and are nearing completion[36] for multijet topologies. Current data on the transverse momentum distributions of $W^{\pm}$ are in good agreement with theoretical expectations.

There are many reasons to be open to the possibility of new gauge bosons:

- High energy parity restoration in an $SU(2)_L \otimes SU(2)_R \otimes U(1)_Y$ electroweak gauge theory;
- The occurrence of extra $U(1)$ gauge symmetries, implying additional Z^0s, for example in unification groups larger than $SU(5)$;
- The low-energy gauge groups emerging from superstring models.

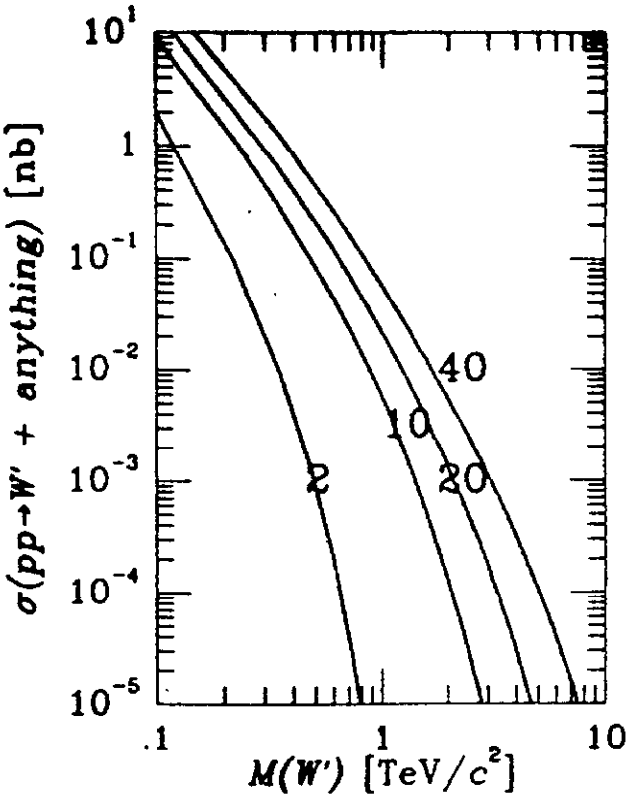

Figure 11: Cross section for the production of a heavy W-boson with rapidity $|y| < 1.5$ in pp collisions at 2, 10, 20, and 40 TeV (after *EHLQ*).

In a specific theory, the style of calculation just described leads to an estimate of the cross section for the production of new gauge bosons. As an example, I show in Fig. 11 the cross section for production of a new W-boson with standard gauge couplings to the light quarks. For the 40 TeV energy projected for the SSC, we may anticipate sensitive searches out to a mass of about 6 TeV/c^2.

Incisive tests of the structure of the electroweak interactions may be achieved in detailed measurements of the cross sections for the production of W^+W^-, $W^\pm Z^0$, Z^0Z^0, $W^\pm\gamma$, and $Z^0\gamma$ pairs. The rate for $W^\pm\gamma$ production is sensitive to the magnetic moment of the intermediate boson. In the standard model there are important cancellations in the amplitudes for W^+W^- and $W^\pm Z^0$ production which rely on the gauge structure of the WWZ trilinear coupling. The Z^0Z^0 and $Z^0\gamma$ reactions do not probe trilinear gauge couplings in the standard model, but are sensitive to nonstandard interactions such as might arise if the gauge bosons were composite. In addition, the W^+W^- and Z^0Z^0 final states may be significant

backgrounds to the detection of heavy Higgs bosons and possible new degrees of freedom.

The intrinsic interest in the process $q_i\bar{q}_i \to W^+W^-$, which accounts in part for plans to study e^+e^- annihilations at c.m. energies around 180 GeV at LEP, is owed to the sensitivity of the cross section to the interplay among the γ-, Z^0-, and quark-exchange contributions. As is well known, in the absence of the Z^0-exchange term, the cross section for production of a pair of longitudinally polarized intermediate bosons is proportional to $\hat{s}$, in gross violation of unitarity. It is important to verify that the amplitude is damped as expected. The mass spectrum of W^+W^- pairs is of interest both for the verification of gauge cancellations and for the assessment of backgrounds to heavy Higgs boson decays. This is shown for intermediate bosons satisfying $|y| < 2.5$ in Fig. 12. The number of pairs produced at high energies seems adequate for a test of the gauge cancellations, provided that the intermediate bosons can be detected with high efficiency.

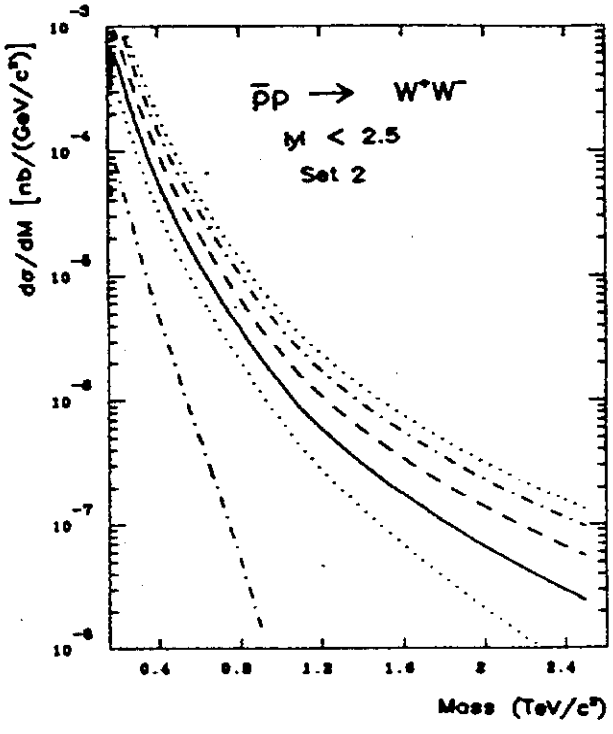

Figure 12: Mass spectrum of W^+W^- pairs produced in pp collisions, according to the standard model and Set 2 of the *EHLQ* parton distributions. Both the W^+ and the W^- must satisfy $|y| < 2.5$.

At this point, it is worth recalling why there must be a physical Higgs boson, or something very similar, in any satisfactory electroweak theory. To do so, let us consider the role of the Higgs boson in the cancellation of high-energy divergences. An illuminating example is provided by the reaction

$$e^+e^- \to W^+W^-, \tag{3.8}$$

which is described in lowest order in the Weinberg-Salam theory by the four Feynman graphs in Fig. 13. The leading divergence in the $J = 1$ amplitude of the neutrino-exchange diagram in Fig. 13(a) is cancelled by the contributions of the direct-channel γ- and Z^0-exchange diagrams. However, the $J = 0$ scattering amplitude, which exists in this case because the electrons are massive and may therefore be found in the "wrong" helicity state, grows as $s^{1/2}$ for the production of longitudinally polarized gauge bosons. The resulting divergence is precisely cancelled by the Higgs boson graph of Fig. 13(d). If the Higgs boson did not exist, we should have to invent something very much like it. From the point of view of S-matrix theory, the Higgs-electron-electron coupling must be proportional to the electron mass, because "wrong helicity" amplitudes are always proportional to the fermion mass.

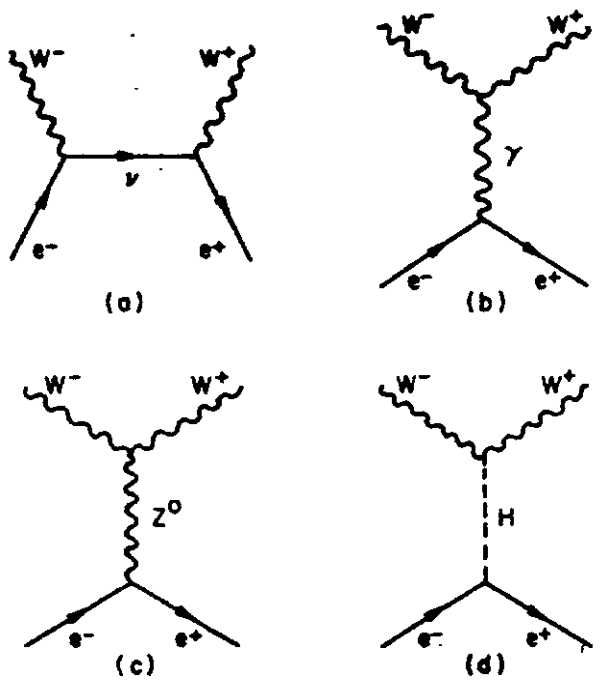

Figure 13: Lowest-order contributions to the reaction $e^+e^- \to W^+W^-$ in the standard model.

Without spontaneous symmetry breaking in the standard model, there would be no Higgs boson, no longitudinal gauge bosons, and no extreme divergence difficulties. (Nor would there be a viable low-energy phenomenology of the weak interactions.) The most severe divergences are eliminated by the gauge structure of the couplings among gauge bosons and leptons. A lesser, but still potentially fatal, divergence arises because the electron has acquired mass – because of the Higgs mechanism. Spontaneous symmetry breaking provides its own cure by supplying a Higgs boson to remove the last divergence. A similar interplay and compensation must exist in any satisfactory theory.

3.3 Heavy Higgs Bosons

We have already remarked that the standard model does not give a precise prediction for the mass of the Higgs boson. We can, however, use arguments of self-consistency to place plausible lower and upper bound on the mass of the Higgs particle in the minimal model. A lower bound is obtained by computing[37] the first quantum corrections to the classical potential

$$V(\phi^\dagger\phi) = \mu_0^2\phi^\dagger\phi + |\lambda|\,(\phi^\dagger\phi)^2\ . \tag{3.9}$$

Requiring that $\langle\phi\rangle \neq 0$ be an absolute minimum of the one-loop potential yields the condition

$$\begin{aligned} M_H^2 &> 3G_F\sqrt{2}(2M_W^4 + M_Z^4)/16\pi^2 \\ &\gtrsim 7\ \mathrm{GeV}/c^2\ . \end{aligned} \tag{3.10}$$

Unitarity arguments[38] lead to a conditional upper bound on the Higgs boson mass. It is straightforward to compute the s-wave partial-wave amplitudes for gauge boson scattering at high energies in the

$$W^+W^-\quad Z^0Z^0\quad HH\quad HZ^0 \tag{3.11}$$

channels. These are all asymptotically constant (*i.e.*, well-behaved), and proportional to $G_FM_H^2$. Requiring that the Born diagrams respect the partial-wave unitarity condition $|a_0| \leq 1$ yields

$$M_H < \left(\frac{8\pi\sqrt{2}}{3G_F}\right)^{1/2} = 1\ \mathrm{TeV}/c^2 \tag{3.12}$$

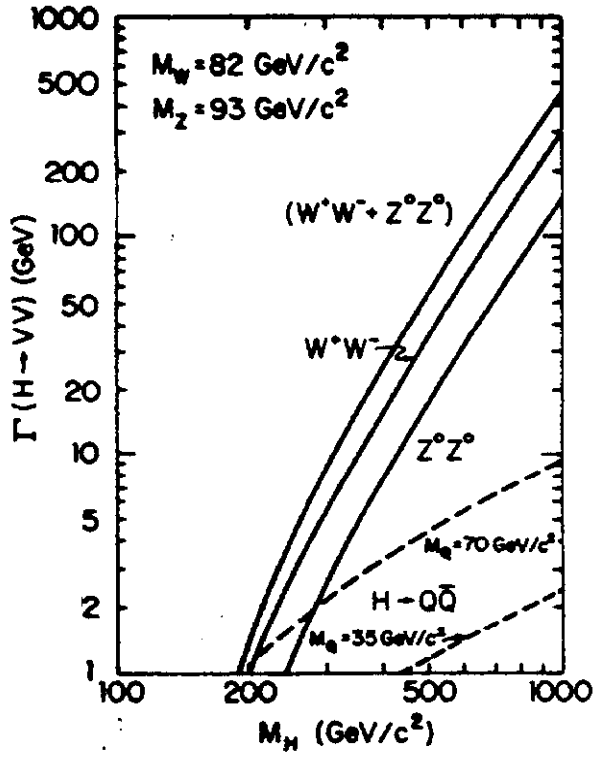

Figure 14: Partial decay widths of the Higgs boson into intermediate boson pairs *vs.* the Higgs-boson mass. For this illustration we have taken $M_W = 82$ GeV/c^2 and $M_Z = 93$ GeV/c^2.

as a condition for perturbative unitarity.

A Higgs boson with $M_H > 2M_W$ has the striking property that it will decay into pairs of gauge bosons. The resulting partial decay widths are shown in Fig. 14, where the partial widths for the decay $H \to Q\overline{Q}$ are also shown for heavy quark masses of 30 and 70 GeV/c^2. The decay into pairs of intermediate bosons is dominant. If the perturbatively estimated width can be trusted, it may be difficult to establish a Higgs boson heavier than about 600 GeV/c^2.

The most promising mechanisms for Higgs boson production are the gluon fusion process[39] and the intermediate boson fusion process.[40] The rate for gluon fusion is sensitive to the masses of the quarks circulating in the loop, and particularly to the top quark mass. I show in Fig. 15 the cross section for W^+W^- pairs

arising in the process

$$pp \rightarrow H + \text{anything} \quad \hookrightarrow W^+W^- \tag{3.13}$$

at $\sqrt{s} = 40$ TeV, as a function of the Higgs boson mass. The rapidities of the W^+ and W^- are restricted to the interval $|y| < 2.5$, and the example shown is for $m_t = 30$ GeV/c^2. The contributions from gluon fusion and intermediate boson fusion are shown separately.

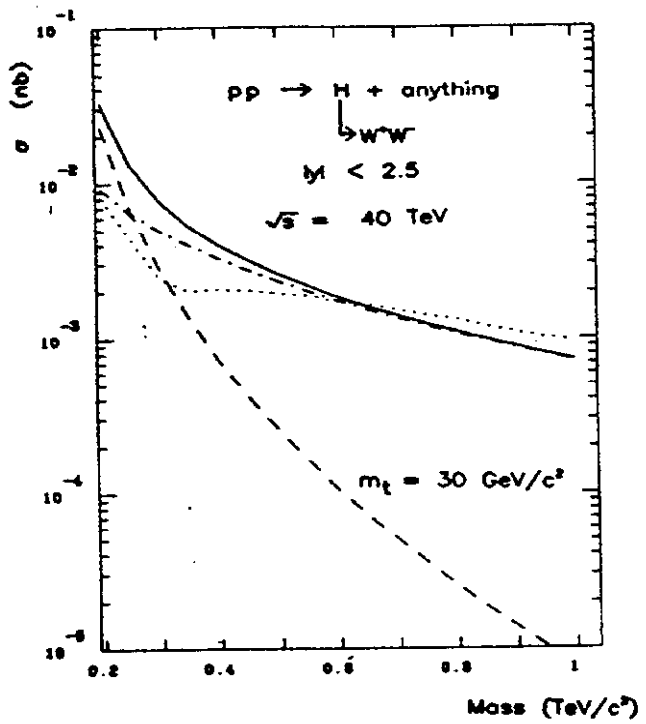

Figure 15: Cross section for the reaction $pp \rightarrow (H \rightarrow W^+W^-) +$ anything, with $m_t = 30$ GeV/c^2, according to the Set 2 parton distributions of *EHLQ*, for $\sqrt{s} = 40$ TeV. The intermediate bosons must satisfy $|y_W| < 2.5$. The contributions of gluon fusion [dashed line] and WW/ZZ fusion [dotted-dashed line] are shown separately. Also shown [dotted line] is $\Gamma_H d\sigma(pp \rightarrow W^+W^- + X)/dM$, with $|y_W| < 2.5$ and $M = M_H$ (*cf.* Fig. 12).

Assuming that the W's can be identified, the background comes from W pair production. We can estimate this background by taking $d\sigma/dM$ for W-pair production with $|y_W| < 2.5$ (Fig. 12) and multiplying by the greater of 10 GeV and the Higgs boson width from Fig. 14. The signal exceeds the background for

$M_H < 630$ GeV/c^2. The signal to background ratio is improved if the top quark is heavier, or if the rapidity cut is tightened to $|y_i| < 1.5$.

From these sorts of comparisons of expected signal and background we can draw the following lessons. First, the rates are reasonably large, even for $m_t = 30$ GeV/c^2, if the $W^\pm$ can be observed with high efficiency. If both W's must be detected in their leptonic decays, the event rates will be down by two orders of magnitude. It is important to study the QCD four-jet background in the final state

$$\begin{array}{ccc} H & \rightarrow & W^+ W^- \\ & & \Big| \quad \hookrightarrow jet_1\, jet_2 \\ & & \hookrightarrow jet_3\, jet_4 \end{array} \tag{3.14}$$

final state. Second, the angular distributions are different for isotropic $H \rightarrow VV$ decay and the forward-backward peaked $q\bar{q} \rightarrow W^+W^-$ reaction. Third, the rate for Higgs production in the Z^0Z^0 mode is one-half the W^+W^- rate, but the standard model background from the process $q\bar{q} \rightarrow Z^0Z^0$ is a factor of five to ten smaller than the corresponding W^+W^- rate. Although the $Z^0 \rightarrow \ell^+\ell^-$ channel may be easy to reconstruct, the price of detecting both Z's in the e^+e^- channel is about three orders of magnitude in rate.

LECTURE 4: TECHNICOLOR

There is at the present time no direct experimental evidence which compels the modification or extension of the standard model. The motivations for going beyond the standard model, or for attempting to "complete" it, are based upon aesthetic principles of theoretical simplicity and elegance, or demands for internal consistency. In this lecture we shall review some of the arguments for elaborating upon the standard model, and will consider the first of several possible extensions: the technicolor scheme of dynamical symmetry breaking. We are not looking for a replacement of the standard model, for we expect that the standard model will remain as the low-energy limit of a more complete theory, much as the four-fermion description of the charged current weak interaction emerges as the low-energy limit of the Weinberg-Salam model.

4.1 WHY THERE MUST BE NEW PHYSICS ON THE 1 TEV SCALE

The standard model is incomplete[41]; it does not explain how the scale of electroweak symmetry breaking is maintained in the presence of quantum corrections. The problem of the scalar sector can be summarized neatly as follows.[42] The Higgs potential of the $SU(2)_L \otimes U(1)_Y$ electroweak theory is

$$V(\phi^\dagger\phi) = \mu_0^2\phi^\dagger\phi + |\lambda|(\phi^\dagger\phi)^2 \,. \tag{4.1}$$

With μ_0^2 chosen less than zero, the electroweak symmetry is spontaneously broken down to the $U(1)$ of electromagnetism, as the scalar field acquires a vacuum expectation value fixed by the low energy phenomenology,

$$< \phi >= \sqrt{-\mu_0^2/2|\lambda|} \equiv (G_F\sqrt{8})^{-1/2} \approx 175 \text{ GeV} \,. \tag{4.2}$$

Beyond the classical approximation, scalar mass parameters receive quantum corrections involving loops containing particles of spins $J = 1, 1/2$, and 0:

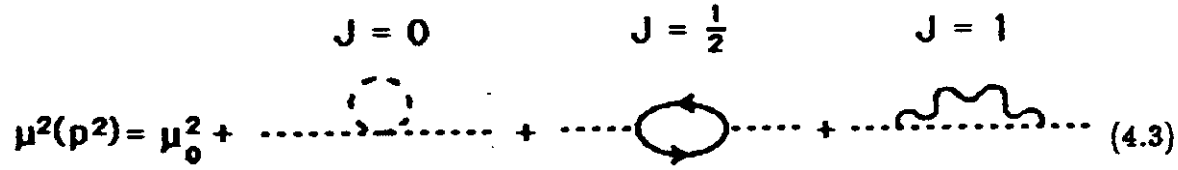

(4.3)

The loop integrals are potentially divergent. Symbolically, we may summarize the content of Eq. (4.3) as

$$\mu^2(p^2) = \mu^2(\Lambda^2) + Cg^2\int_{p^2}^{\Lambda^2} dk^2 + \cdots \,, \tag{4.4}$$

where Λ defines a reference scale at which the value of μ^2 is known, g is the coupling constant of the theory, and C is a constant of proportionality, calculable in any particular theory. Instead of dealing with the relationship between observables and parameters of the Lagrangian, we choose to describe the variation of an observable with the momentum scale. In order for the mass shifts induced by radiative corrections to remain under control (*i.e.*, not to greatly exceed the value measured on the laboratory scale), either

- **Λ must be small, so the range of integration is not enormous; or**

- **new physics must intervene to cut off the integral.**

In the standard $SU(3)_c \otimes SU(2)_L \otimes U(1)_Y$ model, the natural reference scale is the Planck mass,

$$\Lambda \sim M_{\text{Planck}} \approx 10^{19} \text{ GeV} . \tag{4.5}$$

In a unified theory of the strong, weak, and electromagnetic interactions, the natural scale is the unification scale

$$\Lambda \sim M_U \approx 10^{15} \text{ GeV} . \tag{4.6}$$

Both estimates are very large compared to the scale of electroweak symmetry breaking (4.2). We are therefore assured that new physics must intervene at an energy of approximately 1 TeV, in order that the shifts in μ^2 not be much larger than (4.2).

Only a few distinct classes of scenarios for controlling the contribution of the integral in (4.4) can be envisaged. One solution to the problem of the enormous range of integration in (4.4) is offered by theories of dynamical symmetry breaking such as Technicolor.[43] In the technicolor scenario, the Higgs boson is composite, and new physics arises on the scale of its binding, $\Lambda_{TC} \approx O(1 \text{ TeV})$. Thus the effective range of integration is cut off, and mass shifts are under control.

As we shall see, the Technicolor hypothesis also responds to the usual compaints about the standard electroweak theory:

- Arbitrary parameters

  (i) for the Higgs potential;

  (ii) for fermion masses.

- Unnaturalness.

What we mean by the unnaturalness of the standard model is expressed most neatly in an analysis given by 't Hooft.[44] We consider the Lagrangian as an *effective field theory* which describes physics at the shortest distances probed (characterized

by an energy Λ) and at all longer distances in terms of fields appropriate to the scale Λ. In this sense, any Lagrangian we encounter should be thought of as an effective Lagrangian describing physics in terms of the degrees of freedom appropriate to the highest energy scale probed by experiment. In spite of the occasional assertions of some of our visionary colleagues, we can never be certain that we have encountered all the fundamental fields that are to be discovered, up to the highest energies.

What properties must an effective Lagrangian display in order that it can consistently represent the low energy effective interactions of some unknown dynamics acting at a higher energy scale? 't Hooft defines an effective Lagrangian $\mathcal{L}(\Lambda)$ as *natural* at the energy scale Λ if (and only if) every small parameter $\xi \ll \Lambda$ corresponds to a symmetry of $\mathcal{L}(\Lambda)$, *i.e.* if

$$\lim_{\xi \to 0} \mathcal{L}(\Lambda) \tag{4.7}$$

displays additional symmetries. This definition requires no knowledge of physics above the scale Λ. In the standard model, either the Higgs boson mass is large (in which case the unitarity analysis of Lecture 3 shows that the electroweak interactions become strong at energies above 1 TeV) or M_H is small, so that perturbation theory is reliable, but the theory is unnatural. Technicolor eliminates the scalars as fundamental degrees of freedom for $\Lambda \gg G_F^{-1/2}$.

4.2 The Idea of Technicolor

The dynamical symmetry breaking approach, of which technicolor theories are exemplars, is modeled upon our understanding of another manifestation of spontaneous symmetry breaking in Nature, the superconducting phase transition. The macroscopic order parameter of the Ginzburg-Landau phenomenology[45] corresponds to the wave function of superconducting charges. It acquires a nonzero vacuum expectation value in the superconducting state. The microscopic Bardeen-Cooper-Schrieffer theory[46] identifies the dynamical origin of the order parameter with the formation of bound states of elementary fermions, the Cooper pairs of electrons. The basic idea of the technicolor mechanism is to replace the elementary Higgs boson of the standard model by a fermion-antifermion bound state. By analogy with the superconducting phase transition, the dynamics of the fundamental

technicolor gauge interactions among technifermions generate scalar bound states, and these play the role of the Higgs fields.

In the case of superconductivity, the elementary fermions (electrons) and the gauge interactions (QED) needed to generate the scalar bound states are already present in the theory. Could we achieve a scheme of similar economy for the electro weak symmetry breaking transition?

Consider a $SU(3)_c \otimes SU(2)_L \otimes U(1)_Y$ theory of massless up and down quarks. Because the strong interaction is strong, and the electroweak interaction is feeble, we may consider the $SU(2)_L \otimes U(1)_Y$ interaction as a perturbation. For vanishing quark masses, QCD has an exact $SU(2)_L \otimes SU(2)_R$ chiral symmetry. At an energy scale $\sim \Lambda_{QCD}$, the strong interactions become strong, fermion condensates appear, and the chiral symmetry is spontaneously broken

$$SU(2)_L \otimes SU(2)_R \rightarrow SU(2)_V \tag{4.8}$$

to the familiar flavor symmetry. Three Goldstone bosons appear, one for each broken generator of the original chiral invariance. These were identified by Nambu[47] as three massless pions.

The broken generators are three axial currents whose couplings to pions are measured by the pion decay constant f_π. When we turn on the $SU(2)_L \otimes U(1)_Y$ electroweak interaction, the electroweak gauge bosons couple to the axial currents, and acquire masses of order $\sim g f_\pi$. The massless pions thus disappear from the physical spectrum, having become the longitudinal components of the weak gauge bosons. This achieves much of what we desire. Unfortunately, the mass acquired by the intermediate bosons is far smaller than required for a successful low-energy phenomenology; it is only

$$M_W \sim 30 \text{ MeV}/c^2 \,. \tag{4.9}$$

4.3 A MINIMAL MODEL

The simplest transcription of these ideas to the electroweak sector is the minimal technicolor model of Weinberg[48] and Susskind[49]. The technicolor gauge group is taken to be $SU(N)_{TC}$ (usually $SU(4)_{TC}$), so the gauge interactions of the theory

are generated by

$$SU(4)_{TC} \otimes SU(3)_c \otimes SU(2)_L \otimes U(1)_Y \ . \tag{4.10}$$

The technifermions are a chiral doublet of massless color singlets

$$\begin{pmatrix} U \\ D \end{pmatrix}_L \quad U_R,\ D_R \tag{4.11}$$

With the charge assignments $Q(U) = \frac{1}{2}$ and $Q(D) = -\frac{1}{2}$ the theory is free of electroweak anomalies. The ordinary fermions are all technicolor singlets.

In analogy with our discussion of chiral symmetry breaking in QCD, we assume that the chiral TC symmetry is broken,

$$SU(2)_L \otimes SU(2)_R \otimes U(1)_V \to SU(2)_V \otimes U(1)_V \ . \tag{4.12}$$

Three would-be Goldstone bosons emerge. These are the technipions

$$\pi_T^+, \quad \pi_T^0, \quad \pi_T^-; \tag{4.13}$$

for which we are free to *choose* the technipion decay constant as

$$F_\pi = \left(G_F\sqrt{2}\right)^{-1/2} = 247 \text{ GeV} \ . \tag{4.14}$$

When the electroweak interactions are turned on, the technipions become the longitudinal components of the intermediate bosons, which acquire masses

$$\begin{aligned} M_W^2 &= g^2 F_\pi^2/4 &&= \frac{\pi\alpha}{G_F\sqrt{2}\sin^2\theta_W} \\ M_Z^2 &= \left(g^2+g'^2\right)F_\pi^2/4 &&= M_W^2/\cos^2\theta_W \end{aligned} \tag{4.15}$$

that have the canonical standard model values, thanks to our choice (4.14) of the technipion decay constant.

Working by analogy with QCD, we may guess the spectrum of other $F\overline{F}$ bound states as follows:

$$\left.\begin{array}{ll} 1^{--} \text{ technirhos} & \rho_T^+,\ \rho_T^0,\ \rho_T^- \\ 1^{--} \text{ techniomega} & \omega_T \\ 0^{-+} \text{ technieta} & \eta_T \\ 0^{++} \text{ technisigma} & \sigma_T \end{array}\right\} , \tag{4.16}$$

all with masses on the order of the technicolor scale $\Lambda_{TC} \sim O(1\ \mathrm{TeV}/c^2)$, since they do not originate as Goldstone bosons. The dominant decay of the technirho will be

$$\rho_T \rightarrow \pi_T \pi_T \ , \tag{4.17}$$

*i.e.*into pairs of longitudinally polarized gauge bosons. Standard estimates lead to

$$\begin{aligned} M(\rho_T) &\approx 1.77\ \mathrm{TeV}/c^2 \\ \Gamma(\rho_T) &\approx 325\ \mathrm{GeV}\ . \end{aligned} \tag{4.18}$$

Minimal technicolor leads to an enhancement of the cross section for the production of pairs of gauge bosons which we may estimate by applying "technivector meson dominance" to the standard model expressions. I show in Fig. 16 the mass spectrum of W^+W^- pairs produced in pp collisions at 20, 40, and 100 TeV, with and without the technirho enhancement. Both intermediate bosons are required to satisfy $|y| < 1.5$. The technirho enhancement amounts to nearly a doubling of the cross section in the resonance region. However, because the absolute rates are

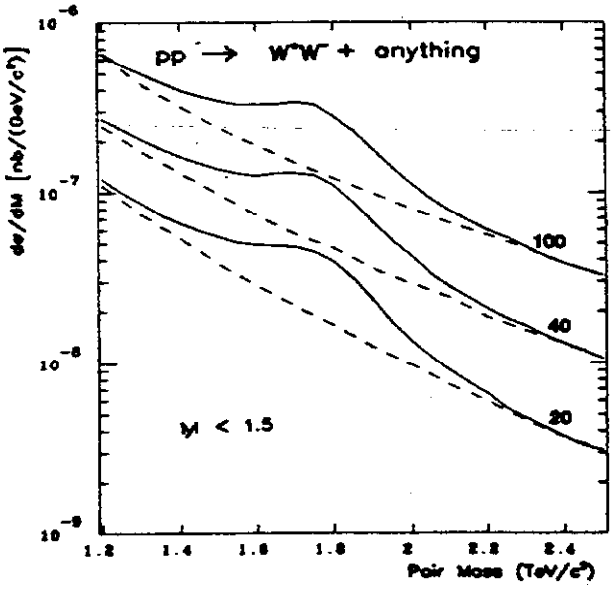

Figure 16: Mass spectrum of W^+W^- pairs produced in pp collisions, according to Set 2 of the *EHLQ* parton distributions. Both W^+ and W^- must satisfy $|y| < 1.5$. The cross sections are shown with (solid lines) and without (dashed lines) the technirho enhancement.

small, the convincing observation of this enhancement is perhaps the most challenging for both collider and experiment that we have encountered. In a standard *SSC* run with integrated luminosity of 10^{40}cm^{-2}, the number of excess events will be 240 on a background of 300 at 40 TeV.

4.4 Extended Technicolor

Technicolor shows how the generation of intermediate boson masses could arise without fundamental scalars or unnatural adjustments of parameters. It thus provides an elegant solution to the naturalness problem of the standard model. However, it has one major deficiency: it offers no explanation for the origin of quark and lepton masses, because no Yukawa couplings are generated between Higgs fields and quarks or leptons.

A possible approach to the problem of quark and lepton masses is suggested by "extended technicolor" models. We imagine that the technicolor gauge group is embedded in a larger extended technicolor gauge group,

$$G_{TC} \subset G_{ETC} , \tag{4.19}$$

which couples quarks and leptons to the technifermions. If the ETC symmetry is spontaneously broken down to the TC symmetry

$$G_{ETC} \to G_{TC} \tag{4.20}$$

at a scale

$$\Lambda_{ETC} \sim 30 - 300 \text{ TeV} , \tag{4.21}$$

then the quarks and leptons may acquire masses

$$m \sim \Lambda_{TC}^3/\Lambda_{ETC}^2 . \tag{4.22}$$

The outlines of this strategy are given in Refs. 50 and 51, but no "standard" ETC model has been constructed.

As a representative of the ETC strategy we may consider a model due to Farhi and Susskind.[52] Their model is built on new fundamental constituents which are analogs of the ordinary quarks (the techniquarks)

$$\begin{pmatrix} U \\ D \end{pmatrix}_L \quad U_R,\ D_R \tag{4.23}$$

and of the ordinary leptons (the technileptons)

$$\begin{pmatrix} N \\ E \end{pmatrix}_L \quad N_R,\ E_R\ . \tag{4.24}$$

These technifermions are bound by the $SU(N)_{TC}$ gauge interaction, which is assumed to become strong at $\Lambda_{TC} \sim 1$ TeV. Among the $F\overline{F}$ bound states are eight color singlet, technicolor singlet pseudoscalar states

$$\left.\begin{array}{ll} \pi_T^+ & (1,1) \\ \pi_T^0 & (1,0) \\ \pi_T^- & (1,-1) \end{array}\right\} \text{become longitudinal } W^\pm,\ Z^0$$

$$\left.\begin{array}{ll} P^+ & (1,1) \\ P^0 & (1,0) \\ P^- & (1,-1) \\ P^{0\prime} & (0,0) \end{array}\right\} \text{pseudo} - \text{Goldstone bosons} \tag{4.25}$$

$$\eta_T' \quad (0,0) \qquad \text{techniflavor singlet}$$

plus the corresponding technivector mesons. Like the η' of QCD, the η_T' couples to an anomalously divergent current, so it is expected to acquire a mass on the order of several hundred GeV/c^2. The pseudo-Goldstone bosons ar massless in the absence of electroweak and ETC interactions.

The possibilities for study of the light particles implied in such a model have been examined recently.[53] There some consequences of the extended technicolor interaction are examined in detail. Here we shall focus instead on pure technicolor aspects, specifically the search for heavy particles, which awaits supercollider experimentation.

In the Farhi-Susskind model, the mass and width of the technirho may be scaled from the known properties of the ρ-meson in QCD. We expect

$$\begin{aligned} M(\rho_T) &\approx 885 \text{ GeV}/c^2 \\ \Gamma(\rho_T) &\approx 500 \text{ GeV} \end{aligned} \tag{4.26}$$

if the technicolor gauge group is $SU(4)_{TC}$. Among technirho enhancements, the most prominent is expected to be in the $W^\pm Z^0$ channel, which will be somewhat easier to observe than the corresponding effect in the minimal model. The resulting mass spectrum is shown in Fig. 17.

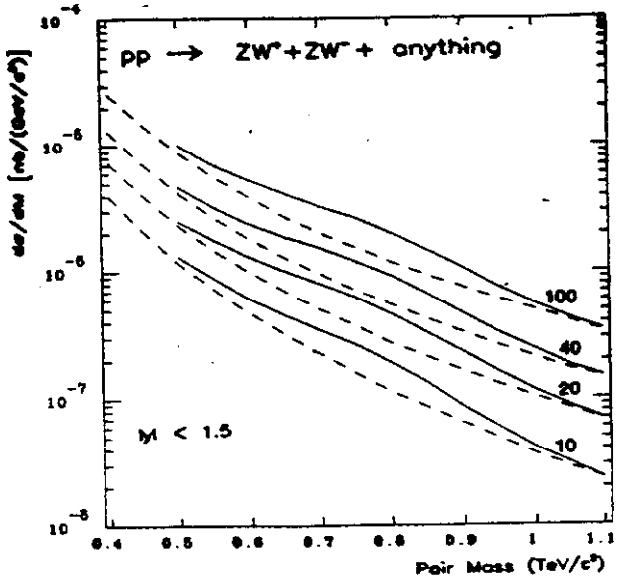

Figure 17: Mass spectrum of $W^{\pm}Z^0$ pairs produced in pp collisions, according to the Farhi-Susskind model (from *EHLQ*). Both intermediate bosons must satisfy $|y| < 1.5$. The cross sections are shown with (solid lines) and without (dashed lines) the technirho (specifically, $\rho_2^{\pm}$) enhancement.

4.5 Colored Technipions

From the color-triplet $(U\ D)$ and color-singlet $(N\ E)$ technifermions, we may build ${}^1S_0$ $(F\overline{F})$ states:

- an isospin triplet P_3^1, P_3^0, P_3^{-1} of color triplets;
- an isospin singlet color triplet state P_3';
- the corresponding antitriplet states;
- an isospin triplet P_8^+, P_8^0, P_8^- of color octets;
- an isoscalar color-octet state $P_8^{0\prime}$,

with masses (acquired from the color interaction) of

$$M(P_3) \approx 160\ \mathrm{GeV}/c^2 \qquad (4.27)$$

$$M(P_8) \approx 240\ \mathrm{GeV}/c^2\ .$$

With the standard charge assignments, the P_8 and P_8' charges are

$$(5/3, 2/3, -1/3; 2/3)\,. \tag{4.28}$$

The isoscalar $P^{0\prime}$ may be produced copiously by gluon-gluon fusion, which leads to equal cross sections in $p^{\pm}p$ collisions. The differential cross section (summed over the eight colors of the produced particle) is

$$\left.\frac{d\sigma(ab \to P_8^{0\prime} + \text{ anything})}{dy}\right|_{y=0} = \frac{5\alpha_s^2}{24\pi F_\pi^2} \cdot \tau f_g^{(a)}(\sqrt{\tau}, M_{P_8}^2) f_g^{(b)}(\sqrt{\tau}, M_{P_8}^2)\,, \tag{4.29}$$

where $\tau = M_P^2/s$ This is shown as a function of the technipion mass in Fig. 18. The dominant decay modes will be

$$P_8^{0\prime} \to \begin{cases} gg \\ t\bar{t} \end{cases}\,. \tag{4.30}$$

The expected branching ratios depend upon the top quark mass, but 50% into each channel is a guess that will not be misleading. In the $t\bar{t}$ channel, the expected signal and background are approximately equal, and the number of events is quite large at supercollider energies. The signal-to-background improves somewhat with

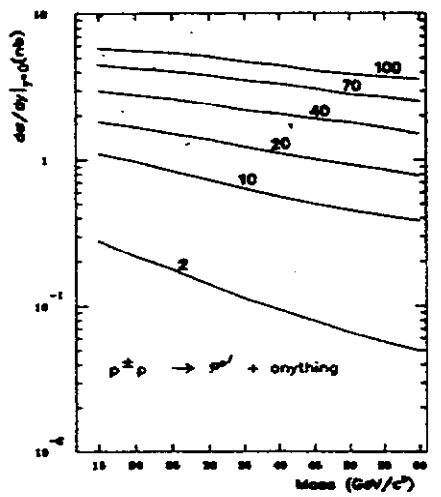

Figure 18: Differential cross section for the production of the color-octet technipion $P_8^{0\prime}$ at $y = 0$ in pp or $\bar{p}p$ collisions at 2, 10, 20, 40, 70, and 100 TeV (from *EHLQ*). The expected mass is approximately 240 GeV/c^2.

increasing technipion mass. The main issues for detection are the identification of t-quarks and the resolution in invariant mass of the reconstructed pairs. This is an appropriate topic for detector studies.

Pairs of colored technipions also will be produced with substantial cross sections at supercollider energies, principally by gluon fusion. As one example, I show in Fig. 19 the integrated cross section for the reaction

$$pp \to P_8\overline{P}_8 \tag{4.31}$$

with and without the technirho ($\rho_8^{0\prime}$) enhancement. These cross sections are typically $\sim$ 15 times the cross sections for color triplet technipion production, and comparable to the cross sections for single $P_8^{0\prime}$ production.

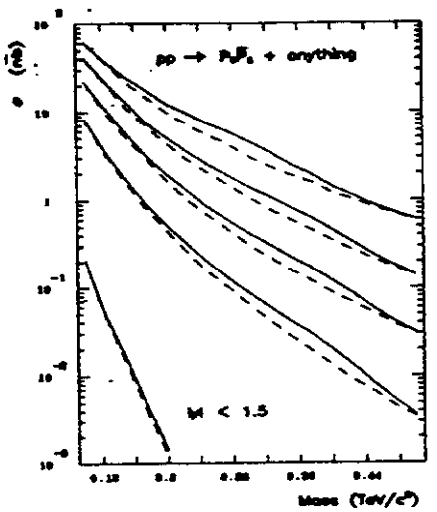

Figure 19: Integrated cross section for the production of $P_8\overline{P}_8$ pairs in pp collisions (from *EHLQ*). Both $P_8^+P_8^-$ and $P_8^0P_8^0+P_8^{0\prime}P_8^{0\prime}$ charge states (which occur with equal cross sections) are summed. Rapidities of the technipions must satisfy $|y| < 1.5$. The cross sections are shown with (solid lines) and without (dashed lines) the technirho enhancement.

The expected decays of octet technipions, in addition to those given in (4.30), are

$$P_8^+ \rightarrow t\bar{b}\,,$$
$$P_8^0 \rightarrow t\bar{t}\,. \tag{4.32}$$

The signature for the $P_8^+ P_8^-$ channel is therefore $t\bar{b}$ on one side of the beam and $\bar{t}b$ on the other. If the heavy flavors can be tagged with high efficiency, we know of no significant conventional backgrounds.

4.6 APPRAISAL

If the technicolor hypothesis correctly describes the breakdown of the electroweak gauge symmetry, there will be a number of spinless technipions with masses below the technicolor scale of about 1 TeV. Some of these, the color singlet, technicolor singlet particles, should be quite light (masses $\lesssim$ 40 GeV) and can be studied using the current generation of e^+e^- and $\bar{p}p$ colliders. The colored particles are probably inacessible to experiment before a supercollider comes into operation, as are technivector mesons. In *EHLQ* we have made a rough appraisal of the minimum effective luminosities required for the observation of various technicolor signals. Full exploitation of the scientific opportunities requires the efficient identification and measurement of heavy quark flavors, and the ability to identify intermediate bosons in complex events. Our expectation is that if the appropriate effort is made in detector development, a 40 TeV collider which supports experimentation at an integrated luminosity of 10^{39}cm^{-2} will be sufficient to confirm or rule out the technicolor hypothesis.

LECTURE 5: SUPERSYMMETRY

We have seen in Lecture 4 that new physics is required on the 1 TeV scale to overcome the problem of uncontrolled mass shifts for the elementary scalars in the theory. There we summarized the one-loop corrections to the scalar mass as

$$\mu^2(p^2) = \mu^2(\Lambda^2) + Cg^2 \int_{p^2}^{\Lambda^2} dk^2 + \cdots , \tag{4.4}$$

where Λ defines a reference scale at which the value of μ^2 is known, g is the coupling constant of the theory, and the coefficient C is calculable in any particular theory. The supersymmetric solution is especially elegant. Exploiting the fact that fermion loops contribute with an overall minus sign (because of Fermi statistics), supersymmetry balances the contributions of fermion and boson loops. In the limit of unbroken supersymmetry, in which the masses of bosons are degenerate with those of their fermion counterparts, the cancellation is exact:

$$\sum_{i=\substack{fermions \\ +bosons}} C_i \int dk^2 = 0 . \tag{5.1}$$

If the supersymmetry is broken (as it must be in our world), the contribution of the integrals may still be acceptably small if the fermion-boson mass splittings ΔM are not too large. The condition that $g^2 \Delta M^2$ be "small enough" leads to the requirement that superpartner masses be less than about 1 TeV/c^2.

5.1 WHAT IS SUPERSYMMETRY?[54]

In relativistic quantum field theory, continuous symmetries of the S-matrix normally are based on Lie algebras. A familiar example is the $SU(2)$ symmetry of isospin, generated by the algebra

$$[T^j, T^k] = i\varepsilon^{jkl} T_l , \tag{5.2}$$

where ε^{jkl} is the antisymmetric three-index symbol. The most general form[55] of symmetries of the S-matrix is the combination of Poincaré invariance plus internal symmetries. The space-time symmetries are generated by the momentum operator P^μ, the generator of translations, and by $M^{\mu\nu}$, the generator of Lorentz boosts and rotations. This leads to the familiar classification of particles by mass and

spin. Internal symmetries are generated by the generators of the symmetry group G, which we denote generically as X_a. These objects commute with the generators of space-time symmetries,

$$\left.\begin{aligned}[X_a, P^\mu] &= 0 \\ [X_a, M^{\mu\nu}] &= 0\end{aligned}\right\}, \tag{5.3}$$

and with the Hamiltonian $\mathcal{H}$ of the world,

$$[X_a, \mathcal{H}] = 0\,, \tag{5.4}$$

so we may simultaneously specify internal quantum numbers along with masses and spins. This leads to the useful classification of particles by representations of the symmetry group G. Examples of internal symmetries are global symmetries such as the flavor symmetries and the $U(1)$ symmetry associated with baryon number conservation, and the local (gauged) symmetries such as $SU(3)_c \otimes SU(2)_L \otimes U(1)_Y$.

The notion of Lie algebras may be generalized to the *graded Lie algebras* defined by both commutators and anticommutators:

$$\left.\begin{aligned}[X, X'] &\sim X'' \\ \{Q, Q'\} &\sim X \\ [Q, X] &\sim Q''\end{aligned}\right\}. \tag{5.5}$$

The generators of the graded Lie algebras are of two kinds. The scalar charges X_a make up the odd part of the algebra, while the spinorial charges Q_a make up the even part. Among the graded Lie algebras, the only ones consistent with relativistic quantum field theory are the supersymmetry algebras,[56] in simplest form

$$\left.\begin{aligned}\{Q_a, \bar{Q}^b\} &\sim \delta_a^b \gamma \cdot P \\ \{Q, Q\} = 0 &= \{\bar{Q}, \bar{Q}\} \\ [P, Q] = 0 &= [P, \bar{Q}]\end{aligned}\right\}, \tag{5.6}$$

where $\bar{Q}$ is the Hermitian conjugate of Q, a and b are internal symmetry labels, and P is a momentum 4-vector.

A particle is transformed by a scalar charge into a partner with the same mass and spin. An example is the action of T_i, which generates isospin rotations about

the i–axis. A particle is transformed by a spinorial charge into a superpartner whose spin differs by 1/2 unit, but otherwise has identical quantum numbers. Thus arises a connection between fermions and bosons.

5.2 The Spectrum of Superpartners

In a supersymmetric theory, particles fall into multiplets which are representations of the supersymmetry algebra. Superpartners share all quantum numbers except spin; if the supersymmetry is unbroken, they are degenerate in mass. The number of fermion states (counted as degrees of freedom) is identical with the number of boson states. In nearly all supersymmetric theories, the superpartners carry a new fermionic quantum number R which is exactly conserved. This means that the lightest superpartner will be absolutely stable. In Table 4 we list the fundamental fields of the standard model and their superpartners. By examining the quantum numbers of known particles, we readily see that there are no candidates for supersymmetric pairs among them. Supersymmetry therefore means doubling the particle spectrum, compared with the standard model. In fact, we must expand the spectrum slightly further, because the minimal supersymmetric extension of the standard model requires at least two doublets of Higgs bosons.[57] The interactions among old and new particles are prescribed by the supersymmetric extension of the usual interaction Lagrangian, which we shall take to be the $SU(3)_c \otimes SU(2)_L \otimes U(1)_Y$ theory. If supersymmetry is an invariance of the Lagrangian, it is evidently a broken symmetry, because observationally boson masses are not equal to the masses of their fermion counterparts. For supersymmetry to resolve the hierarchy problem, we have seen that it must be effectively unbroken above the electroweak scale of $O(1\ \mathrm{TeV})$. This suggests that superpartner masses will themselves be $\lesssim 1\ \mathrm{TeV}/c^2$.

There is no convincing theory for masses of the superpartners. (This is not worse than the situation for the masses of the usual fermions or scalars.) As for the ordinary particles, however, we can derive relations among superparticle masses, and infer restrictions on the masses. Three kinds of indirect methods yield interesting relations:

Table 4: Fundamental Fields of the Standard Model and their Superpartners

Particle	Spin	Color	Charge
g gluon	1	8	0
$\tilde{g}$ gluino	1/2	8	0
γ photon	1	0	0
$\tilde{\gamma}$ photino	1/2	0	0
$W^{\pm}, Z^0$ intermediate bosons	1	0	$\pm 1, 0$
$\tilde{W}^{\pm}, \tilde{Z}^0$ wino and zino	1/2	0	$\pm 1, 0$
q quark	1/2	3	2/3, -1/3
$\tilde{q}$ squark	0	3	2/3, -1/3
e electron	1/2	0	-1
$\tilde{e}$ selectron	0	0	-1
ν neutrino	1/2	0	0
$\tilde{\nu}$ sneutrino	0	0	0
$H^+ \quad H'^0$ $H^0 \quad H'^-$ Higgs bosons	0	0	$\pm 1, 0$
$\tilde{H}^+ \quad \tilde{H}'^0$ $\tilde{H}^0 \quad \tilde{H}'^-$ Higgsinos	1/2	0	$\pm 1, 0$

- The role of virtual superpartners in rare processes. An example within the standard model is the limit on the $m_c - m_u$ mass splitting inferred from the magnitude of the $K^0 - \overline{K}^0$ transition amplitude.

- Cosmological constraints. A standard model example is the bound on the sum of light neutrino masses inferred from the limits on the mass density of the Universe.

- The distortion of standard model predictions. A conventional example is the bound on the number of light neutrino species inferred from the total width of the Z^0.

It is instructive to consider one example of each of these approaches.

Barbieri and collaborators[58] have studied the deviations from quark–lepton universality in charged-current weak interactions that would arise from the exchange of superpartners. In lowest contributing order, corrections to the muon decay rate are due to diagrams containing sleptons and gauginos, whereas corrections to the β–decay rate are due to diagrams containing squarks and gauginos. The requirement that the Fermi constant inferred from β–decay agree with that determined from muon decay within experimental errors, so that

$$\left|\frac{\delta G^{\beta}}{G^{\beta}} - \frac{\delta G^{\mu}}{G^{\mu}}\right| < 2 \times 10^{-3} , \tag{5.7}$$

then leads to constraints on the squark-slepton mass difference. These are quite restrictive if the wino mass is small ($\lesssim M_W/2$). If the wino mass is comparable to the W-boson mass, this calculation suggests that deviations from universality are to be found just inside the present experimental limits.

Constraints on the mass of a stable photino may be derived from the observed mass density of the Universe using methods[59] developed to bound the masses of stable neutrinos. If the photino is light, it is straightforward to compare the contribution of photinos to the mass density of a 2.7–K Universe,

$$\rho_{\tilde{\gamma}} \approx 109\, m_{\tilde{\gamma}}\ \mathrm{cm}^{-3} \tag{5.8}$$

with the critical (closure) density

$$\rho_{crit} = (3.2 - 10.3)(\mathrm{keV}/c^2)\mathrm{cm}^{-3} \tag{5.9}$$

(a reasonable upper bound on the observed density), to find

$$m_{\tilde{\gamma}} \lesssim 100\ \mathrm{eV}/c^2 . \tag{5.10}$$

When the photino mass exceeds about 1 MeV/c^2, it is necessary to take into account the annihilation of photinos into light fermions by the exchange of a scalar partner of the fermions. The results of this analysis[60] yield a lower bound on the mass of a "heavy" photino, which is shown together with (5.10) in Fig. 20.

Gauge boson decays may within a few years provide useful sources of superpartners. The principal decays are given in Table 5. These have interesting consequences for

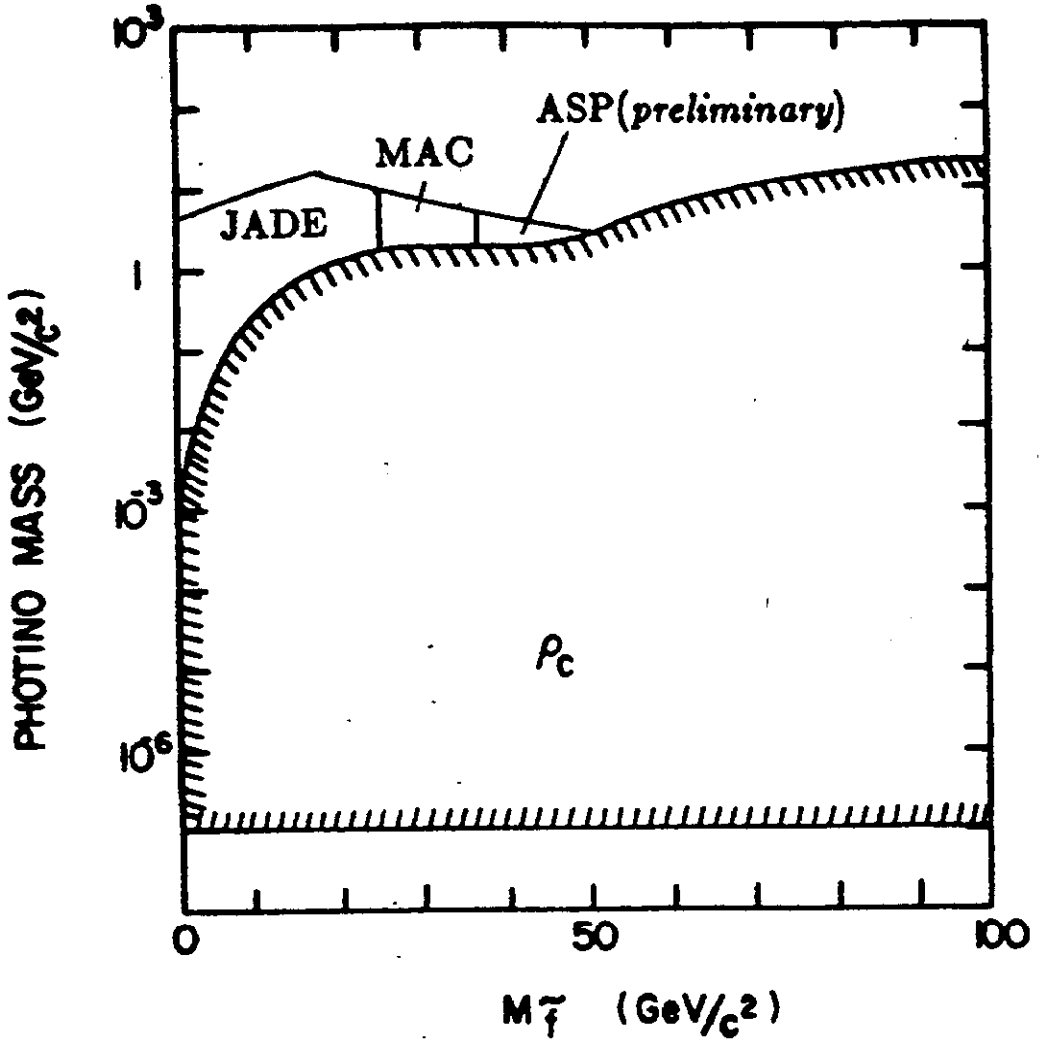

Figure 20: Cosmological limits on the allowed photino mass as a function of the mass of the lightest scalar partner of a charged fermion. The photino is assumed to be stable, and the lightest superparticle. Shown for comparison are the limits from three accelerator experiments (Refs. 61–63).

- Direct searches, e.g.

$$W \rightarrow \tilde{e}\tilde{\nu} \quad \hookrightarrow e\tilde{\gamma} \tag{5.11}$$

- The widths of W and Z;

- Distortion of the ratio

$$R \equiv \frac{\sigma(\bar{p}p \rightarrow W^{\pm} + \text{anything})B(W \rightarrow e\nu)}{\sigma(\bar{p}p \rightarrow Z^0 + \text{anything})B(Z^0 \rightarrow e^+e^-)} . \tag{5.12}$$

Table 5: Gauge Boson Decays as Sources of Superpartners

$W^{\pm}$	Z^0
Decay Modes	
$\tilde{\omega}_i\tilde{\gamma}$	$\tilde{\omega}_i^+\tilde{\omega}_j^-$
$\tilde{\omega}_i\tilde{Z}^0$	$\tilde{Z}\tilde{H}$
$\tilde{\omega}_i\tilde{H}^0$	$\tilde{q}\bar{\tilde{q}}^*$
$\tilde{q}\bar{\tilde{q}}'^*$	$\tilde{\ell}^+\tilde{\ell}^-$
$\tilde{\ell}\tilde{\nu}$	$\tilde{\nu}\bar{\tilde{\nu}}^*$

We denote by $\tilde{\omega}_i$ the mass eigenstates resulting from $\tilde{W} - \tilde{H}$ mixing. Mixing among both charged and neutral gauginos and higgsinos is treated in detail by Dawson, *et al.*, Ref. 54.

The last of these has been analyzed recently by Deshpande, et al.[64] QCD corrections to the "Drell-Yan" production cross sections are believed to cancel to good approximation in the ratio, so that knowledge of the proton structure functions implies a prediction of R which depends upon the branching ratios for leptonic decay. The ratio grows as the number of light neutrino species is increased, or as generations of superpartners are added. Typical expectations are shown in Fig. 21. The experimental results

$$R = \begin{cases} 9.6^{+3.0}_{-2.1} & [\mathrm{UA}-1]^{65} \\ 7.35^{+1.78}_{-2.16} & [\mathrm{UA}-2]^{66} \end{cases} \tag{5.13}$$

must still be regarded as provisional, because of the limited statistics on Z^0-production. Clearly interesting limits on the number of light neutrino species and useful constraints on the superpartner spectrum will soon emerge.

We have already noted that there is no convincing theory for the masses of superpartners. Indeed, even the *ordering* of superpartner masses is quite model dependent. What this means for direct searches is that one must consider all reasonable possibilities. In practice, this entails

- Searching for all superpartners;
- Considering all plausible decay modes of each one;

- **Making use of existing experimental constraints.**

It is generally expected that the photino $\tilde{\gamma}$ is the lightest superpartner, and hence is stable. If global supersymmetry is spontaneously broken, the theory acquires a massless Goldstone *fermion*, the Goldstino $\tilde{\mathcal{G}}$. Decays of the form

$$\tilde{\gamma} \rightarrow \gamma \tilde{\mathcal{G}} \tag{5.14}$$

are then allowed. In supergravity theories, based upon spontaneously broken *local* supersymmetry, the Goldstino becomes the helicity $\pm 1/2$ components of the mas-

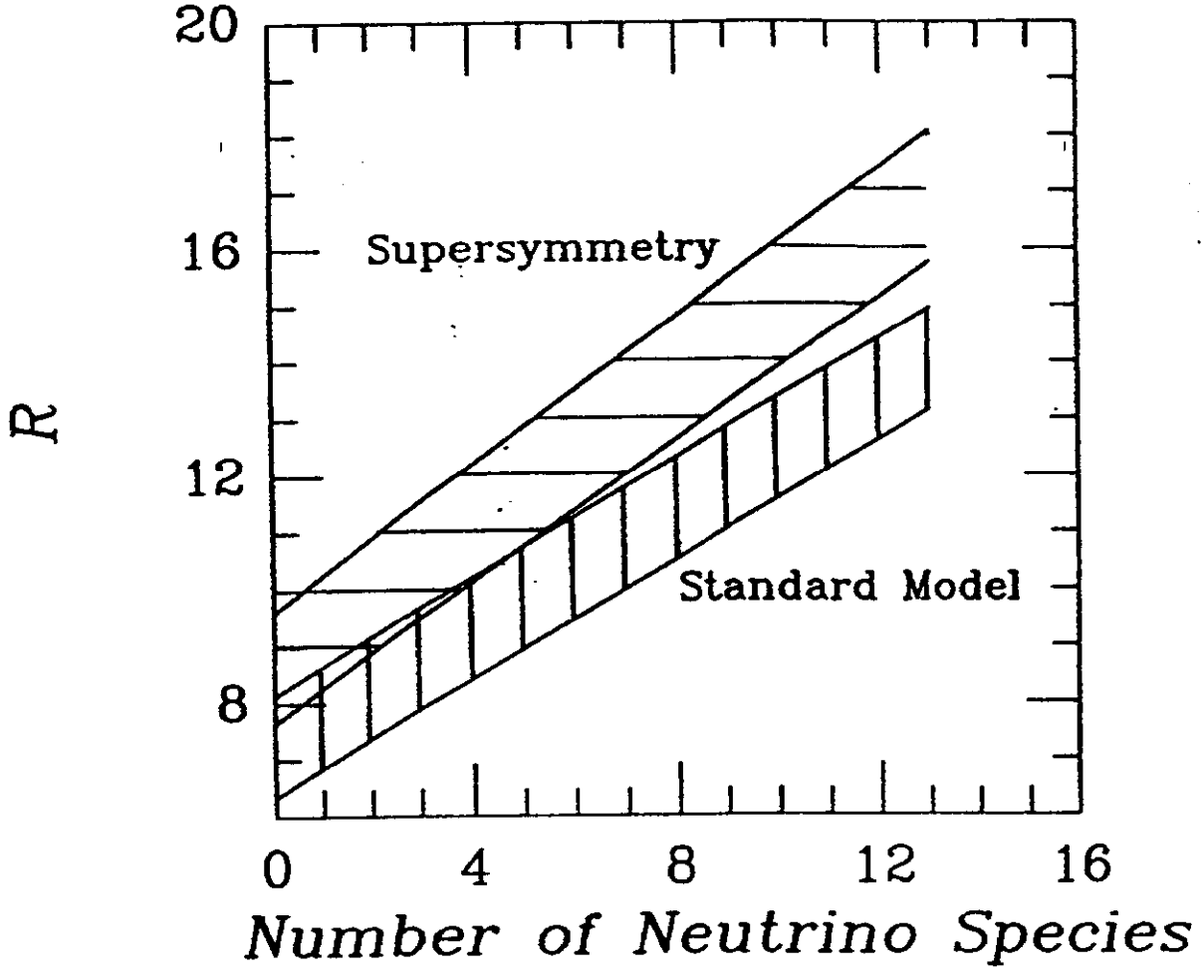

Figure 21: The ratio R defined in eqn. (5.12) versus the number of light neutrino species (after Deshpande, et al., Ref. 64). The upper band gives the result for a supersymmetry model, with parameters chosen to maximize the effect. The lower band shows the result for the standard model. I have enlarged the uncertainties to better reflect ambiguities in the structure functions.

sive, spin-3/2 gravitino, and is not available as a decay product of a light photino. The other popular candidate for the lightest superpartner is the *sneutrino*, $\tilde{\nu}$. Any of these candidates is a weakly interacting neutral particle, which will result in undetected energy. Although it is important to consider all possibilities systematically, we shall assume for most of today's discussion that the lightest superpartner is the photino.

The strongly interacting superparticles are of particular interest because they are produced at substantial rates in hadron-hadron collisions. Possible decay chains and signatures for squarks and gluinos are indicated in Fig. 22. For each unstable strongly interacting superpartner produced, we expect one, two, or three jets, accompanied by missing energy.

Before we turn to our main subject, the search for supersymmetry at high energies, it will be useful to have in mind a rough summary of the limits on masses of superpartners as they stand before the analysis of data from the $S\bar{p}pS$ collider. I caution that every entry hangs on assumptions about decay chains, *etc.*, and that few categorical statements are reliable. For thorough discussions of the limits, see the papers by Haber and Kane, and by Dawson, *et al.*, in Ref. 4. An abbreviated statement of existing limits is given in Table 6.

Table 6: Limits on the Masses of Superpartners

Particle	Limit
$\tilde{\gamma}$	could be as light as a few GeV/c^2, or massless
$\tilde{g}$	could be as light as a few GeV/c^2
$\tilde{W}$	$\gtrsim$ 25 GeV/c^2 for massless $\tilde{\gamma}$ and $\tilde{\nu}$
$\tilde{Z}$	$>$ 41 GeV/c^2 for massless $\tilde{\gamma}$ and $M(e) = 22$ GeV/c^2 (but see Fig. 21)
$\tilde{q}$	if stable: $>$ 14 GeV/c^2; if unstable (and photino is massless): $>$ 17.8 GeV/c^2 for $e_{\tilde{q}} = 2/3$; 3 GeV/$c^2 \lesssim M \lesssim$ 7.4 GeV/c^2 or $\gtrsim$ 16 GeV/c^2 for $e_{\tilde{q}} = -1/3$
$\tilde{\ell}^{\pm}$	$\gtrsim$ 20 GeV/c^2

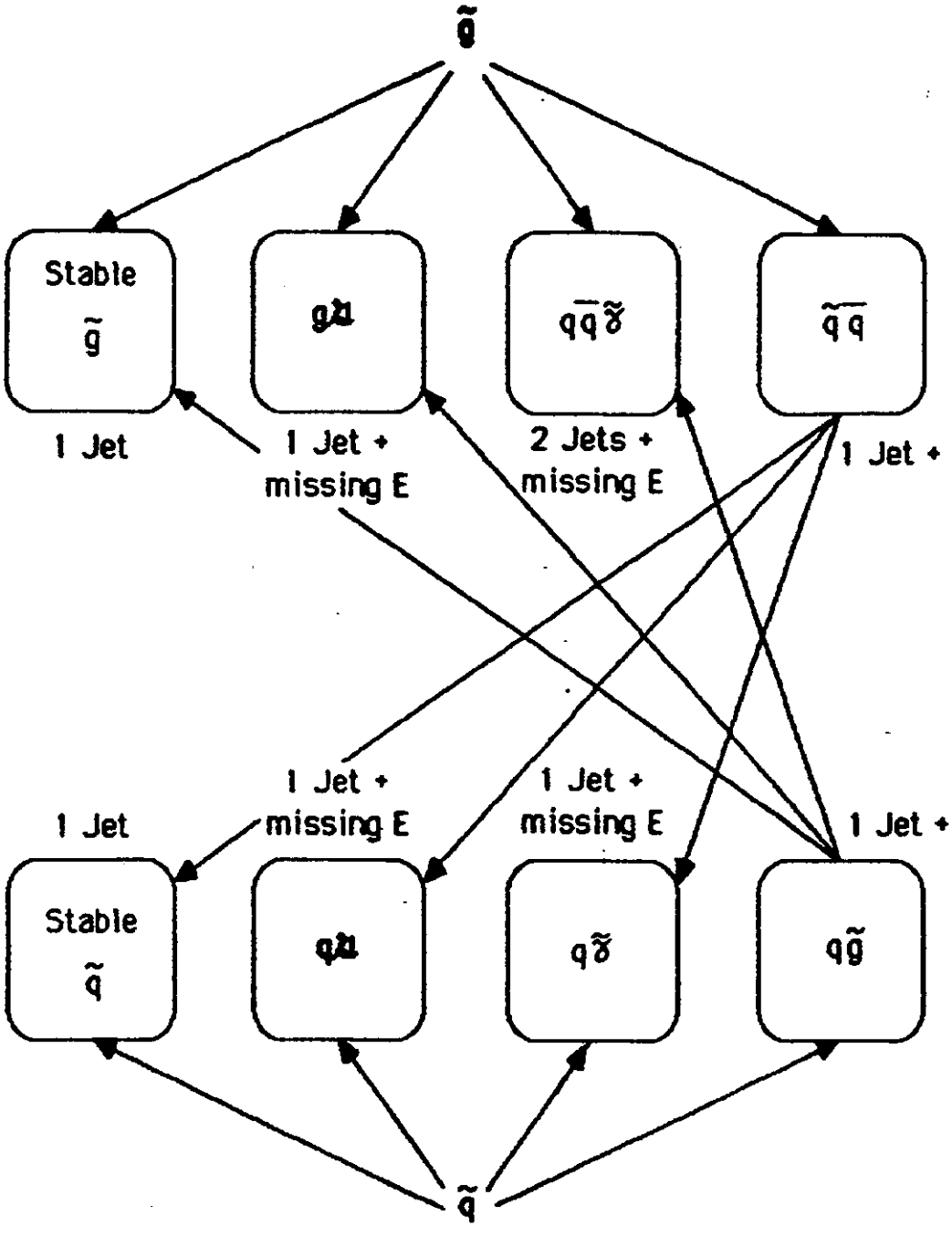

Figure 22: Signatures of the strongly interacting superpartners.

5.3 SUPERPARTICLE SEARCHES IN $p^{\pm}p$ COLLISIONS

Over the past few years, a great deal of effort has gone into estimating production rates for superpartners. Sally Dawson, Estia Eichten, and I[54] have evaluated all the lowest–order (Born diagram) cross sections $d\hat{\sigma}/d\hat{t}$ and $\hat{\sigma}$ for the production of

$$(\tilde{q}, \tilde{\ell}^{\pm}, \tilde{\nu}, \tilde{g}, \tilde{\gamma}, \tilde{Z}^0, \tilde{H}^0, \tilde{H}^{0\prime}, \tilde{W}^{\pm}, \tilde{H}^{\pm})^2 \tag{5.15}$$

final states in parton–parton collisions, including the possibility of mixing among $(\tilde{\gamma}, \tilde{Z}, \tilde{H}^0, \tilde{H}^{0\prime})$ or $(\tilde{W}^{\pm}, \tilde{H}^{\pm})$. We have also calculated the processes initiated by e^+e^- collisions. Many of these reactions have been studied by others as well; complete references are given in our paper. The approximate magnitudes of the cross sections are indicated in Table 7.

The outlines of the search for supersymmetry at the SSC are given in *EHLQ*.[1] Progress since Snowmass '84 was summarized recently at the Oregon workshop by Dawson.[67] Cross sections for the production of superpartners should be quite ample for a luminosity of 10^{32} cm^{-2}sec^{-1} or more, and a c.m. energy of 40 TeV. As examples, I show in Figs. 23–25 the integrated cross sections for the production of superpartners with rapidities $|y_i| < 1.5$, for the reactions

$$pp \to \tilde{g}\tilde{g} + \text{anything}, \tag{5.16}$$

$$pp \to \tilde{g}\tilde{q} + \text{anything}, \tag{5.17}$$

and

$$pp \to \tilde{g}\tilde{\gamma} + \text{anything}, \tag{5.18}$$

Table 7: Hierarchy of Superpartner Production Rates

Final States	Mechanism	Magnitude
$(\tilde{g}, \tilde{q})^2$	QCD	α_s^2
$(\tilde{g}, \tilde{q}) \cdot (\tilde{\gamma}, \tilde{Z}^0, \tilde{H}^0, \tilde{H}^{0\prime}, \tilde{W}^{\pm}, \tilde{H}^{\pm})$	electroweak/QCD	$\alpha \cdot \alpha_s$
$\tilde{\ell}\tilde{\nu}, \tilde{\ell}\tilde{\ell}^*, \tilde{\nu}\tilde{\nu}^*$	decay of $W^{\pm}, Z^0$ virtual $W^{\pm}, Z^0$	α α^2
$(\tilde{\gamma}, \tilde{Z}^0, \tilde{H}^0, \tilde{H}^{0\prime}, \tilde{W}^{\pm}, \tilde{H}^{\pm})^2$	electroweak	α^2

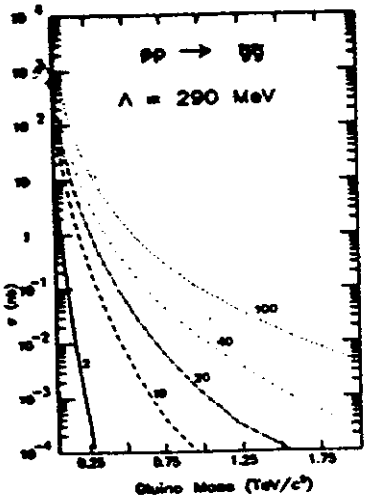

Figure 23: Cross sections for the reaction $pp \to \tilde{g}\tilde{g}$ + anything as a function of gluino mass, for collider energies $\sqrt{s} = 2$, 10, 20, 40, and 100 TeV, according to the *EHLQ* parton distributions (Set 2). Both gluinos are restricted to the interval $|y_i| < 1.5$. For this illustration, the squark mass is set equal to the gluino mass. [From Ref. 1.]

respectively.

On the basis of these and other cross section calculations and a rudimentary assessment of the requirements for detection, we have estimated the discovery limits for various energies and luminosities. These estimates are shown in Table 8 for gluinos, squarks, photinos, zinos, winos, and sleptons. We infer from these estimates that a 40–TeV $p^{\pm}p$ collider with integrated luminosity exceeding 10^{39} cm^{-2} should be adequate to establish the presence or absence of the superpartners predicted by models of low–energy supersymmetry.

5.4 CONCLUSIONS

We have examined a general class of supersymmetric theories in which the effective low–energy theory relevant at 1 TeV or below is the supersymmetric extension of $SU(3)_c \otimes SU(2)_L \otimes U(1)_Y$. The search for supersymmetry is complicated by the absence of reliable predictions for the masses of superpartners. Low–energy

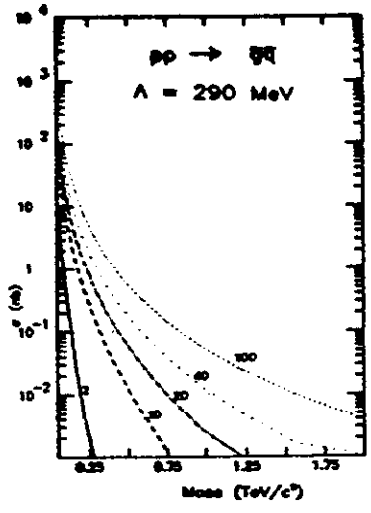

Figure 24: Cross sections for the reaction $pp \to \tilde{g}(\tilde{q}_u$ or $\tilde{q}_d$ or $\tilde{q}_u^*$ or $\tilde{q}_d^*) +$ anything as a function of the superparticle mass for collider energies $\sqrt{s} = 2$, 10, 20, 40, and 100 TeV, according to the *EHLQ* parton distributions (Set 2). We have assumed equal masses for the squarks and gluino, and have included the partners of both left–handed and right–handed quarks. Both squark and gluino are restricted to the rapidity interval $|y_i| < 1.5$. [From Ref. 1.]

supersymmetry is surprisingly unconstrained by experiment, in spite of increasing efforts over the past two years. For example, gluinos and photinos as light as a few GeV/c^2 are allowed for some ranges of parameters, in all scenarios. Interesting limits can be placed on *stable* squarks and sleptons. For *unstable* scalar quarks, stringent limits exist only if the photino is massless.

A complete catalogue of total and differential cross sections exists for the production of superpartners in $p^{\pm}p$ and e^+e^- collisions. Detailed simulations, including detector characteristics, are required; important work along these lines is in progress, but continued iteration with experimental reality will be needed. At the $S\bar{p}pS$ and Tevatron Colliders, rates are ample for superpartner masses up to about 100 GeV/c^2, but good signatures beyond the traditional "missing E_T" tag must be devised. The SSC will permit the study of squarks and gluinos up to masses of 1 Tev/c^2 and beyond.

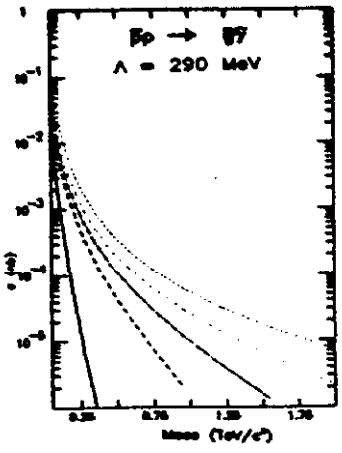

Figure 25: Cross sections for the reaction $pp \to \tilde{g}\tilde{\gamma}$ + anything as a function of the photino mass, for $\sqrt{s} = 2$, 10, 20, 40, and 100 TeV. Both gluino and photino are restricted to the rapidity interval $|y_i| < 1.5$. All squark and gaugino masses are taken to be equal. [From *EHLQ*.]

Table 8: Expected discovery limits for superpartners from associated production of squarks and gauginos in 40 TeV pp collisions. All superpartner masses are set equal.

	Mass limit [GeV/c^2]		
$\int dt\mathcal{L}$ [cm^{-2}]	10^{38}	10^{39}	10^{40}
Superpartner			
Gluino (1000 events)	900	1,600	2,500
Squark ($\tilde{u} + \tilde{d}$) (1000 events)	800	1,450	2,300
Photino (100 events)	350	750	1,350
Zino (1000 events)	250	500	825
Wino (1000 events)	300	550	1,000

LECTURE 6: COMPOSITENESS

Throughout these lectures, we have assumed the quarks and leptons to be elementary point particles. This is consistent with the experimental observations to date that the "size" of quarks and leptons is bounded from above by

$$R < 10^{-16} \text{ cm} . \tag{6.1}$$

Indeed, the identification of quarks and leptons as elementary particles (whether that distinction holds at all distance scales or only the regime we are now able to explore) is an important ingredient in the simplicity of the standard model.

We may nevertheless wish to entertain the possibility that the quarks and leptons are themselves composites of some still more fundamental structureless particles, for the followeing reasons:

- The proliferation of "fundamental" fermions

$$\begin{array}{llll} \begin{pmatrix} u \\ d \end{pmatrix}_L & \begin{pmatrix} c \\ s \end{pmatrix}_L & \begin{pmatrix} [t] \\ b \end{pmatrix}_L & u_R, d_R, s_R, c_R, b_R, [t_R] \\ \begin{pmatrix} \nu_e \\ e \end{pmatrix}_L & \begin{pmatrix} \nu_\mu \\ \mu \end{pmatrix}_L & \begin{pmatrix} \nu_\tau \\ \tau \end{pmatrix}_L & e_R, \mu_R, \tau_R \end{array} \tag{6.2}$$

  and the repetition of generations.

- The complex pattern of masses and angles suggests they may not be fundamental parameters.

- Hints of a new strong interaction (Technicolor) and the resulting composite scalar particles.

To this we may add the most potent question of all, Why not?

6.1 A PROTOTYPE THEORY OF COMPOSITE QUARKS OR LEPTONS

Building on our knowledge of gauge theories for the interactions of fundamental fermions, we imagine[68] a set of massless, pointlike, spin-1/2 *preons* carrying

the charge of a new gauge interaction called *metacolor*. The metacolor interaction arises from a gauge symmetry generated by the group $\mathcal{G}$. We assume that the metacolor interaction is asymptotically free and infrared confining. Below the characteristic energy scale Λ^*, the metacolor interaction become strong (in the sense that $\alpha_M(\Lambda^{*2}) \approx 1$) and binds the preons into metacolor-singlet states including the observed quarks and leptons. In this way, the idea of composite quarks and leptons may be seen as a natural extension of the technicolor strategy for composite Higgs scalars.

We expect from the small size of the quarks and leptons that the characteristic energy scale for preon confinement must be quite large,

$$\Lambda^* \gtrsim 1/R \ . \tag{6.3}$$

On this scale, the quarks and leptons are effectively massless. This is the essential fact that a composite theory of quarks and leptons must explain: the quarks and leptons are both small and light.

In general, it is the scale Λ^* which determines the masses of composite states. However, there are special circumstances in which some composite states will be exactly or approximately massless compared to the scale Λ^*. The Goldstone theorem[69] asserts that a massless spin-zero particle arises as a consequence of the spontaneous breakdown of a continuous global symmetry. We have already seen examples of this behavior in the small masses of the color-singlet technipions, which arise as Goldstone bosons when the chiral symmetry of tecchnicolor is spontaneously broken.

't Hooft noted that under certain special conditions, confining theories which possess global chiral symmetries may lead to the existence of massless composite fermions when the chiral symmetries are not spontaneously broken. The key to this observation is the anomaly condition[70] which constrains the pattern of chiral symmetry breaking and the spectrum of light composite fermions:

> For any conserved global (flavor) current, the same anomaly must arise from the fundamental preon fields and from the "massless" physical states.

The existence of an anomaly therefore implies a massless physical state associated with the anomalous charge Q. If the (global) chiral or flavor symmetry respected by the preons is broken down when the metacolor interaction becomes strong as

$$G_f \to S_f \subseteq G_f \text{ at } \Lambda^* \ , \tag{6.4}$$

then the consistency condition can be satisfied in one of two ways:

- If the anomalous charge $Q \notin S_f$, so the global symmetry which has the anomaly is spontaneously broken, then a Goldstone boson arises with specified couplings to the anomaly;
- If instead $Q \in S_f$, so that the anomalous symmetry remains unbroken when metacolor becomes strong, then there must be massless, spin-1/2 fermions in the physical spectrum which couple to Q and reproduce the anomaly as given by the preons.

The anomaly conditions thus show how massless fermions might arise as composite states in a strongly interacting gauge theory. In analogy with the case of the pions, we may then suppose that a small bare mass for the preons, or preon electroweak interactions that explicitly break the chiral symmetries, can account for the observed masses of quarks and leptons. However, there is as yet no realistic model of the quark and lepton spectrum. It is natural to ask whether the repeated pattern of generations might be an excitation spectrum. The answer seems clearly to be No. For a strong gauge interaction, all the excitations should occur at a scale Λ^* and above.

The scenario which emerges from this rather sketchy discussion of composite models is that all quarks and leptons are massless in some approximation. Generations arise not from excitations, but because of symmetries coupled with the anomaly condition. All masses and mixings arise because of symmetry breaking not associated with the composite strong force. This is a promising outcome on two out of three counts: We may hope for some insight into the near masslessness of quarks and leptons, and into the meaning of generations, but the origin of mass and mixings seems as mysterious as ever.

6.2 MANIFESTATIONS OF COMPOSITENESS

The classic test for substructure is to search for form factor effects, or deviations from the expected pointlike behavior in gauge-boson propagators and fermion vertices.[71] Such deviations would occur in any composite model, at values of $\sqrt{\hat{s}} \gg \Lambda^*$, for example as a consequence of vector meson dominance. In a favored parametrization of this effect, the gauge field propagator is modified by a factor

$$F(Q^2) = 1 + Q^2/\Lambda^{*2} \ , \tag{6.5}$$

where Q is the four-momentum carried by the gauge field. Measurements of the reactions

$$e^+e^- \to \begin{cases} q\bar{q} \\ \ell^+\ell^- \end{cases} \tag{6.6}$$

yield limits on the compositeness scale which translate into the bound on fermion size given in (6.1).

Many other tests of compositeness can be carried out in the study at low energies of small effects or rare transitions sensitive to virtual processes. For example, if a composite fermion f is naturally light because of 't Hooft's mechanism, there will arise a contribution to its anomalous magnetic moment of order[72] $(m_f/\Lambda^*)^2$. The close agreement[73] between the QED prediction and the measured value of $(g-2)_\mu$ implies that

$$\Lambda^* \gtrsim 670 \text{ GeV} \tag{6.7}$$

for the muon. This is the only constraint on Λ^* from anomalous moments that improves on the limits from the reactions (6.6). Within specific models, very impressive bounds on the compositeness scale may be derived from the absence of flavor-changing neutral current transitions.

At energies below those for which form factor effects become characteristic, *i.e.* for

$$\sqrt{\hat{s}} \sim \text{ few times } \Lambda^*, \tag{6.8}$$

we may anticipate resonance formation and multiple production. The latter might

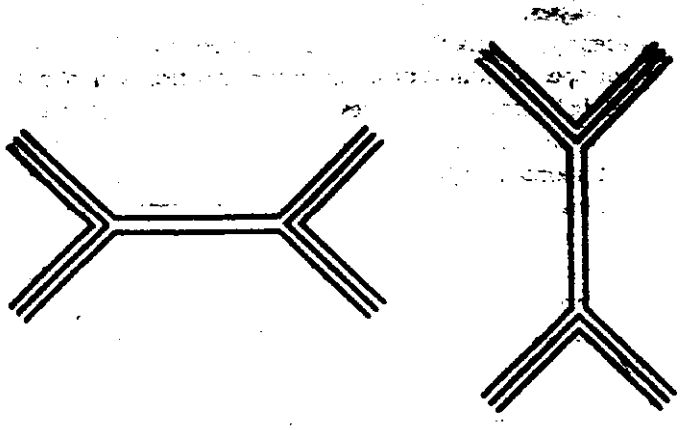

Figure 26: Typical elastic interaction of composite fermions mediated by the exchange of preon bound states with masses of order Λ^*.

well include reactions such as

$$u\bar{u} \rightarrow \begin{cases} u\bar{u}u\bar{u} \\ u\bar{u}e\bar{e} \\ q^*\bar{q}^* \end{cases} , \tag{6.9}$$

etc. In some ways, these would be the most direct and dramatic manifestations of compositeness.

At energies small compared to the compositeness scale, the interaction between bound states is governed by the finite size of the bound states, by the radius R. Because the interactions are strong only within this confinement radius, the cross section for scattering composite particles at low energies should be essentially geometric,

$$\sigma \sim 4\pi R^2 \sim 4\pi/\Lambda^{*2} . \tag{6.10}$$

Regarded instead in terms of the underlying field theory, the low energy interaction will be an effective four-fermion interaction, mediated by the exchange of massive bound states of preons, as shown in Fig. 26. When

$$\sqrt{\hat{s}} \ll \Lambda^*, \tag{6.11}$$

the resulting interaction will be a contact term, similar to the low-energy limit of the electroweak theory. The general form of the contact interaction will be

$$\mathcal{L}_{contact} \sim \frac{g^2_{Metacolor}}{M_V^2} \cdot \bar{f}_4 \gamma_\mu f_2 \bar{f}_3 \gamma^\mu f_1 . \tag{6.12}$$

Identifying $M_V \approx \Lambda^*$ and

$$g_M^2/4\pi = 1\,, \tag{6.13}$$

we see that this interaction reproduces the expected geometrical size of the cross section in the limit (6.11).

6.3 Signals for Compositeness in $p^{\pm}p$ Collisions

The flavor-diagonal contact interactions symbolized by (6.12) will modify the cross sections for ff elastic scattering. If in the standard model this process is controlled by a gauge coupling $\alpha_f \ll 1$, then the helicity-preserving pieces of the contact interaction give rise to interference terms in the integrated cross section for ff scattering that are of order[74]

$$\frac{\hat{s}}{\Lambda^{*2}} \cdot \frac{g^2}{4\pi\alpha_f} \equiv \frac{\hat{s}}{\alpha_f \Lambda^{*2}} \tag{6.14}$$

relative to the standard model contribution. This modification to the conventional expectation is far more dramatic than the anticipated $O(\hat{s}/\Lambda^{*2})$ form factor effects. The direct contact term itself will dominate for (sub)energies satisfying

$$\hat{s} \gtrsim \alpha_f \Lambda^{*2}\ . \tag{6.15}$$

The approximation that the composite interactions can be represented by contact terms can of course only be reasonable when (6.11) is satisfied.

Although various flavor-changing contact interactions can be tuned away in particular models (and must be, in many cases, to survive experimental constraints), the flavor-diagonal contact interactions that originate in the exchange of common preons must in general survive. This suggests a strategy for testing the idea of compositeness:

> Consider only four-fermion interactions which are flavor-preserving and respect the $SU(3)_c \otimes SU(2)_L \otimes U(1)_Y$ gauge symmetry of the standard model.

These are unavoidable in a theory capable of producing massless fermionic bound states. Three cases are to be considered:

- **electron compositeness;**
- **quark compositeness;**
- **common lepton-quark compositeness.**

The second and third, which can be attacked effectively in hadron-hadron collisions, will be our concern here.

In the case of quark-quark scattering, we look for deviations from the consequences of QCD for the production of hadron jets. We have seen in Lecture 2 that QCD gives a generally good account of the jet cross sections observed at the $S\overline{p}pS$. However, there are higher-order QCD effects which remain to be fully understood, and practical observational questions that depend upon details of fragmentation, and hence on nonperturbative effects. For all these reasons, it is necessary to observe a rather large and characteristic deviation to identify it as a sign of compositeness.

The most general contact interactions that respect the gauge symmetry of the standard model, involve only up and down quarks, and are helicity preserving, involve ten independent terms. In *EHLQ*we have analyzed the consequences of one of these as an example of the phenomena to be anticipated in a composite world:

$$\mathcal{L}^{(0)}_{contact} = \eta_0 \cdot \frac{g^2}{2\Lambda^{*2}} \overline{q}_L \gamma^\mu q_L \overline{q}_L \gamma_\mu q_L \ , \tag{6.16}$$

where $g^2/4\pi \equiv 1$ and $\eta_0 = \pm 1$. This interaction modifies the amplitudes for the transitions

$$\begin{gathered} u\overline{u} \to u\overline{u} \quad d\overline{d} \to d\overline{d} \\ uu \to uu \quad dd \to dd \quad \overline{u}\overline{u} \to \overline{u}\overline{u} \quad \overline{d}\overline{d} \to \overline{d}\overline{d} \\ u\overline{u} \to d\overline{d} \\ ud \to ud \quad u\overline{d} \to u\overline{d} \quad \overline{u}d \to \overline{u}d \\ \overline{u}\overline{d} \to \overline{u}\overline{d} \end{gathered} \tag{6.17}$$

but has no effect on processes involving gluons.

It is convenient to write the differential cross section for the parton-parton scatteing process as

$$\frac{d\hat{\sigma}(ij \to i'j')}{d\hat{t}} = \frac{\pi}{\hat{s}^2} |A(ij \to i'j')|^2 \ . \tag{6.18}$$

Then in the presence of a contact term (6.16) the squares of amplitudes are

$$\begin{aligned} |A(ud \to ud)|^2 &= \left|A(u\bar{d} \to u\bar{d})\right|^2 \\ &= |A(\bar{u}d \to \bar{u}d)|^2 = \left|A(\bar{u}\bar{d} \to \bar{u}\bar{d})\right|^2 \qquad (6.19) \\ &= \frac{4}{9}\alpha_s^2(Q^2)\frac{\hat{s}^2+\hat{u}^2}{\hat{t}^2} + \left[\frac{\eta_0\hat{u}}{\Lambda^{*2}}\right]^2 \ ; \end{aligned}$$

$$\begin{aligned} \left|A(u\bar{u} \to d\bar{d})\right|^2 &= \left|A(d\bar{d} \to u\bar{u})\right|^2 \\ &= \frac{4}{9}\alpha_s^2(Q^2)\frac{\hat{t}^2+\hat{u}^2}{\hat{u}^2} + \left[\frac{\eta_0\hat{u}}{\Lambda^{*2}}\right]^2 \ ; \qquad (6.20) \end{aligned}$$

$$\begin{aligned} |A(u\bar{u} \to u\bar{u})|^2 &= \left|A(d\bar{d} \to d\bar{d})\right|^2 \\ &= \frac{4}{9}\alpha_s^2(Q^2)\left[\frac{\hat{u}^2+\hat{s}^2}{\hat{t}^2} + \frac{\hat{u}^2+\hat{t}^2}{\hat{s}^2} - \frac{2\hat{u}^2}{3\hat{s}\hat{t}}\right] \qquad (6.21) \\ &\quad + \frac{8}{9}\alpha_s(Q^2)\frac{\eta_0}{\Lambda^{*2}}\left[\frac{\hat{u}^2}{\hat{t}} + \frac{\hat{u}^2}{\hat{s}}\right] + \frac{8}{3}\left[\frac{\eta_0\hat{u}}{\Lambda^{*2}}\right]^2 \ ; \end{aligned}$$

$$\begin{aligned} |A(uu \to uu)|^2 &= |A(dd \to dd)|^2 \\ &= |A(\bar{u}\bar{u} \to \bar{u}\bar{u})|^2 = \left|A(\bar{d}\bar{d} \to \bar{d}\bar{d})\right|^2 \qquad (6.22) \\ &= \frac{4}{9}\alpha_s^2(Q^2)\left[\frac{\hat{u}^2+\hat{s}^2}{\hat{t}^2} + \frac{\hat{s}^2+\hat{t}^2}{\hat{u}^2} - \frac{2\hat{s}^2}{3\hat{u}\hat{t}}\right] \qquad (6.23) \\ &\quad + \frac{8}{9}\alpha_s(Q^2)\frac{\eta_0}{\Lambda^{*2}}\left[\frac{\hat{s}^2}{\hat{t}} + \frac{\hat{s}^2}{\hat{u}}\right] + \left[\frac{\eta_0}{\Lambda^{*2}}\right]^2\left(\hat{u}^2+\hat{t}^2+\frac{2}{3}\hat{s}^2\right) \ . \end{aligned}$$

Relative to the QCD terms, the influence of the contact term grows linearly with the square $\hat{s}$ of the parton-parton subenergy.

I show in Fig. 27 the differential cross section $d\sigma/dp_\perp dy\,|_{y=0}$ for the reaction

$$pp \to \text{jet} + \text{anything} \qquad (6.24)$$

that follow from these amplitudes.

The gross features of these curves are easily understood. Because the contact term modifies the cross section for (anti)quark–(anti)quark scattering, its effects

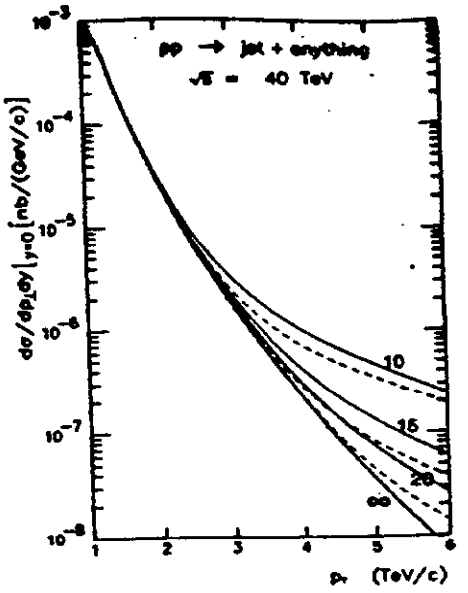

Figure 27: Cross section $d\sigma/dp_\perp dy\ |_{y=0}$ for jet production in pp collisions at $\sqrt{s} = 40$ TeV (from *EHLQ*). The curves are labeled by the compositeness scale Λ^* (in TeV). $\eta_0 = -1$: solid lines; $\eta_0 = +1$: dashed lines.

are most apparent at the large values of $p\perp$ for which valence quark interactions dominate the jet cross section.

To estimate what limits can be set on the compositeness scale, we must adopt a plausible discovery criterion. We require that in a bin of width $\Delta p_\perp = 100$ GeV/c, the deviation

$$\Delta(p_\perp) = \frac{\left.\frac{d\sigma}{dp_\perp dy}\right|_{y=0} - \left.\frac{d\sigma^{QCD}}{dp_\perp dy}\right|_{y=0}}{\left.\frac{d\sigma^{QCD}}{dp_\perp dy}\right|_{y=0}} \tag{6.25}$$

correspond to a factor-of-two change in the cross section, with at least 50 events observed per unit rapidity. The resulting limits on Λ^* are shown in Fig. 28. We see that at 40 TeVand 10^{40} cm^{-2}, a pp collider can probe scales of 15-20 TeV.

The $S\overline{p}pS$ experiments have already been able to set interesting limits on the compositeness scale for quarks.[75] Typical results of the current generation of experiments are shown in Fig. 29. On the basis of these early, low-luminosity

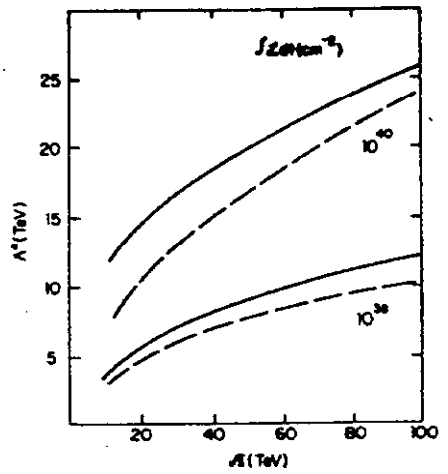

Figure 28: Maximum compositeness scale Λ^* probed in jet production at $y = 0$ in pp collisions as a function of $\sqrt{s}$ for integrated luminosities of 10^{40} and 10^{38} cm^{-2}. The solid lines correspond to $\eta_0 = -1$, the dashed lines to $\eta_0 = +1$.

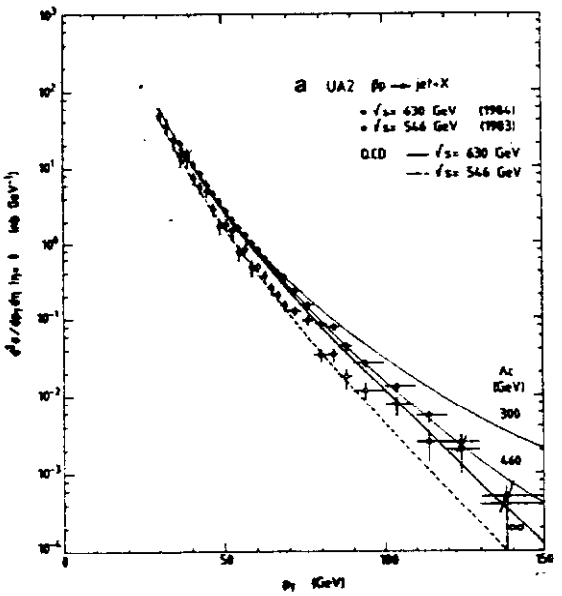

Figure 29: Inclusive jet production cross sections from the UA-2 experiment, Ref. 75. The data points correspond to collision energies $\sqrt{s} = 630$ GeV (full circles) and $\sqrt{s} = 546$ GeV (open circles). The curves show QCD calculations, including (at 630 GeV) the influence of a contact term.

measurements, we may already conclude that

$$\Lambda^* \gtrsim 300 \text{ GeV} \ . \tag{6.26}$$

A similar analysis for Bhabha scattering angular distributions leads to limits on the order of 1–2 TeV for the compositeness scale of the electron.

If quarks and leptons have a common preon constituent, the familiar Drell-Yan contribution to dilepton production will be modified by a contact term. The effects of such an additional contribution are illustrated in Fig. 30, for the reaction

$$pp \to \ell^+\ell^- + \text{ anything} \tag{6.27}$$

at 40 TeV. Whereas the conventional Drell-Yan contribution falls rapidly with M (because both parton luminosities and the elementary cross section do), the cross sections including the contact interaction have nearly flattened out. The weak dependence upon the effective mass of the lepton pair results from the convolution of the rising elementary cross section with the falling parton luminosities. There are no conventional backgrounds to this signal for quark and lepton substructure.

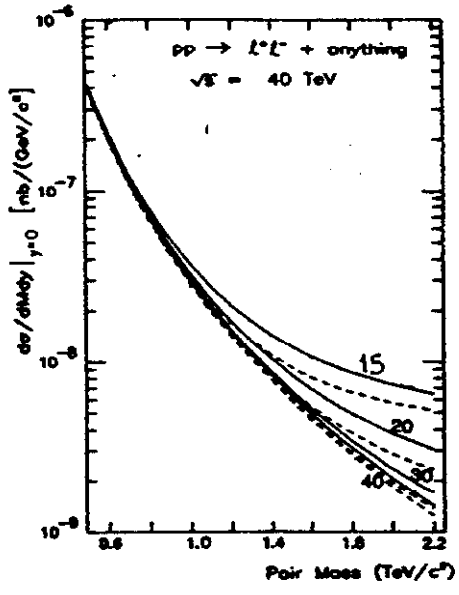

Figure 30: Cross section $d\sigma/dMdy\ |_{y=0}$ for dilepton productin in pp collisions at $\sqrt{s} = 40$ TeV (from *EHLQ*). The curves are labeled by the compositeness scale Λ^* (in TeV). The solid (dashed)lines correspond to a negative (positive) sign for the contact term.

The contributions of contact terms to dilepton production and jet production ar comparable. However, in jet production there are large incoherent QCD contributions from quark-gluon and gluon-gluon interactions. In addition, the standard model cross section for $q\bar{q} \to \ell^+\ell^-$ is smaller than the quark-quark scattering cross section by a factor of order $(\alpha_{EM}/\alpha_s)^2$. This accounts for the greater prominence of the compositeness signal in dilepton production. We estimate that the study of lepton pairs at the *SSC* will be sensitive to compositeness scales on the order of 26 TeV.

EPILOGUE

The advances of the past decade have brought us tantalizingly close to a profound new understanding of the fundamental constituents of matter and the interactions among them. Progress toward a fuller synthesis surely requires both theoretical and experimental breakthroughs. While many ideas may precede the definitive experiments, it is likely that theoretical insights will require the impetus of experimental discovery. Though we do not know what the future holds, we may be confident that important clues are to be found on the scale of 1 TeV, and that a multi-TeV hadron supercollider will supply the means to reveal them.

ACKNOWLEDGEMENTS

It is a pleasure to thank Spenta Wadia and his colleagues on the Organizing Committee for their tireless efforts to ensure the success of the Panchgani Winter School. My collaborators Estia Eichten, Ian Hinchliffe, and Ken Lane have contributed mightily to my appreciation of the scientific potential of a supercollider. Fermilab is operated by Universities Research Association, Inc., under contract with the United States Department of Energy.

FOOTNOTES AND REFERENCES

[1] E. Eichten, I. Hinchliffe, K. Lane, and C. Quigg, *Rev. Mod. Phys.* **56**, 579 (1984).

[2] Basic references on supercollider physics include the following: *Proceedings of the 1984 Summer Study on Design and Utilization of the Superconducting Super Collider,* edited by R. Donaldson and J. G. Morfín (Fermilab, Batavia, Illinois, 1984); *Large Hadron Collider in the LEP Tunnel,* edited by G. Brianti, *et al.*, CERN 84-10; *Proceedings of the Workshop on Electroweak Symmetry Breaking,* edited by T. Appelquist, M. K. Gaillard, and I. Hinchliffe, LBL-18571; $\bar{p}p$ *Options for the Supercollider,* edited by J. E. Pilcher and A. R. White (University of Chicago, 1984); *Physics at the Superconducting Super Collider Summary Report,* edited by P. Hale and B. Winstein (Fermilab, 1984); *Supercollider Physics,* edited by D. E. Soper (World Scientific, Singapore, 1986); E. Eichten, Fermilab-Pub-85/178-T.

[3] For a summary of this thinking, see, for example, O. W. Greenberg, *Phys. Today* **38**, No. 9, p. 22 (September, 1985).

[4] M. M. Block and R. N. Cahn, *Rev. Mod. Phys.* **57**, 563 (1985).

[5] G. Altarelli and G. Parisi, *Nucl. Phys.* **B126**, 298 (1977).

[6] H. Abramowicz, *et al.*, *Z. Phys.* *C***13**, 199 (1982); *C***17**, 283 (1983).

[7] For example, D. B. MacFarlane, *et al.*, *Z. Phys.* *C***26**, 1 (1984). The forthcoming CDHS analysis itself implies a larger sea distribution than before (A. Para, private communication).

[8] The original data on the EMC effect are given in J. J. Aubert, *et al.*, *Phys. Lett.* **123B**, 275 (1983).

[9] A. Bodek, *et al.*, *Phys. Rev.* *D***20**, 1471 (1979).

[10] J. J. Aubert, *et al.*, *Phys. Lett.* **123B**, 123 (1983).

[11] J. C. Collins and Wu-Ki Tung, Fermilab-Pub-86/39–T.

[12] E. Eichten, I. Hinchliffe, K. Lane, and C. Quigg, Fermilab-Pub-86/75–T.

[13] J. L. Ritchie, in *Proceedings of the 1984 Summer Study on Design and Utilization of the Superconducting Super Collider,* edited by R. Donaldson and J. G. Morfin (Fermilab, Batavia, Illinois, 1984), p. 237.

[14] S. J. Brodsky, J. C. Collins, S. D. Ellis, J. F. Gunion, and A. H. Mueller, *ibid.*, p. 227.

[15] L. V. Gribov, E. M. Levin, and M. G. Ryskin, *Phys. Rep.* **100**, 1 (1983).

[16] A. H. Mueller and Jianwei Qiu, "Gluon Recombination and Shadowing at Small Values of x," Columbia preprint CU–TP–322.

[17] J. C. Collins, in *Proceedings of the 1984 Summer Study on Design and Utilization of the Superconducting Super Collider,* edited by R. Donaldson and J. G. Morfin (Fermilab, Batavia, Illinois, 1984), p. 251.

[18] G. J. Hanson, *et al.*, *Phys. Rev. Lett.* **35**, 1609 (1975).

[19] See, for example, S. M. Berman, J. D. Bjorken, and J. B. Kogut, *Phys. Rev.* *D*4, 3388 (1971).

[20] For early results, see G. Arnison, *et al..*, *Phys. Lett.* **132B**, 214 (1983); P. Bagnaia, *et al.*, *Z. Phys.* *C*20, 117 (1983).

[21] R. K. Ellis and J. C. Sexton, Fermilab-Pub-85/152-T.

[22] The elementary cross sections have been calculated by many authors. Convenient summaries are given in *EHLQ* and in J. F. Owens, E. Reya, and M. Glück, *Phys. Rev.* *D*18, 1501 (1978).

[23] R. N. Cahn, in *Proceedings of the 10th SLAC Summer Institute,* edited by Anne Mosher, SLAC Report No. 259, p. 1.

[24] W. Scott, in *Proceedings of the Interrnational Symposium on Physics of Proton-Antiproton Collision,* edited by Y. Shimizu and K. Takikawa (KEK, National Laboratory for High Energy Physics, Tsukuba, 1985), p. 68.

[25] G. Arnison, *et al.* (UA-1 Collaboration), CERN-EP/86-29.

[26] The curves shown are 1.5× the lowest-order QCD predictions, evaluated with $Q^2 = p_\perp^2$. The systematic errors on the data are ±70%. Theoretical uncertainties are of a similar magnitude, but tend to increase the predicted cross section. These are discussed by Eichten, *et al.*, Ref. 1, and by Ellis and Sexton, Ref. 21.

[27] G. Sterman and S. Weinberg, *Phys. Rev. Lett.* **39**, 1436 (1977).

[28] K.-I. Shizuya and S.-H. H. Tye, *Phys. Rev. Lett.* **41**, 787 (1978); M. B. Einhorn and B. G. Weeks, *Nucl. Phys.* **B146**, 445 (1978).

[29] B. L. Combridge, *Nucl. Phys.* **B151**, 429 (1979).

[30] Z. Kunszt, E. Pietarinen, and E. Reya, *Phys. Rev.* *D***21**, 73 (1980).

[31] P. de Causmaecker, R. Gastmans, W. Troost, and T. T. Wu, *Nucl. Phys.* **B206**, 53 (1982).

[32] S. Parke and T. Taylor, *Phys. Lett.* **157B**, 81 (1985).

[33] S. Parke and T. Taylor, Fermilab-Pub-85/118-T, 85/162-T; L. Chang, Z. Xu, D.-H. Zhang, Tsinghua University Preprints TUTP-84/3, 84-4, 84-5; Z. Kunszt, CERN preprint TH.4319/85.

[34] For a detailed introduction, see C. Quigg, *Gauge Theories of the Strong, Weak, and Electromagnetic Interactions,* Benjamin/Cummings, 1983. A more elementary treatment is given by I. J. R. Aitchison and A. J. G. Hey, *Gauge Theories in Particle Physics,* Adam Hilger, 1982.

[35] G. Altarelli, R. K. Ellis, and G. Martinelli, *Z. Phys.* **C27**, 617 (1985).

[36] W. J. Stirling, R. Kleiss, and S. D. Ellis, CERN preprint TH.4209/85; S. D. Ellis, R. Kleiss, and W. J. Stirling, *Phys. Lett.* **154B**, 435 (1985); *Phys. Lett.* **158B**, 341 (1985); J. Gunion, Z. Kunszt, and M. Soldate, *Phys. Lett.* **163B**, 389 (1985).

[37] A. D. Linde, *Zh. Eksp. Teor. Fiz. Pis'ma Red.* **23**, 73 (1976) [*JETP Lett.* **23**, 64 (1976)]; S. Weinberg, *Phys. Rev. Lett.* **36**, 294 (1976).

[38] B. W. Lee, C. Quigg, and H. B. Thacker, *Phys. Rev.* *D***16**, 1519 (1977).

[39] H. Georgi, S. L. Glashow, M. E. Machacek, and D. V. Nanopoulos, *Phys. Rev. Lett.* **40**, 692 (1978).

[40] R. N. Cahn and S. Dawson, *Phys. Lett.* **136B**, 196 (1984).

[41] For a summary of the standard shortcomings, see E. Eichten, I. Hinchliffe, K. Lane, and C. Quigg, Ref. 1.

[42] M. Veltman, *Acta Phys. Polon.* *B***12**, 437 (1981); C. H. Llewellyn Smith, *Phys. Rep.* **105**, 53 (1984).

[43] For reviews of the technicolor idea, see E. Farhi and L. Susskind, *Phys. Rep.* **74**, 277 (1981); R. Kaul, *Rev. Mod. Phys.* **55**, 449 (1983). A recent study for the current generation of accelerators appears in E. Eichten, I. Hinchliffe, K. D. Lane, and C. Quigg, Fermilab-Pub-85/145-T, *Phys. Rev. D,* (to be published).

[44] G. 't Hooft, in *Recent Developments in Gauge Theories,* edited by G. 't Hooft, *et al.* (Plenum, New York, 1980), p. 135.

[45] V. L. Ginzburg and L. D. Landau, *Zh. Eksp. Teor. Fiz.* **20**, 1064 (1950).

[46] J. Bardeen, L. N. Cooper, and J. R. Schrieffer, *Phys. Rev.* **106**, 162 (1962).

[47] Y. Nambu, *Phys. Rev. Lett.* **4**, 380 (1960).

[48] S. Weinberg, *Phys. Rev.* *D***13**, 974 (1976), *ibid.* **19**, 1277 (1979).

[49] L. Susskind, *Phys. Rev.* *D***20**, 2619 (1979).

[50] S. Dimopoulos and L. Susskind, *Nucl. Phys.* **B155**, 237 (1979).

[51] E. Eichten and K. Lane, *Phys. Lett.* **90B**, 125 (1980).

[52] E. Farhi and L. Susskind, *Phys. Rev.* *D***20**, 3404 (1979).

[53] Eichten, *et al.*, Ref. 43.

[54] A systematic development is given in J. Wess and J. Bagger, *Supersymmetry and Supergravity* (Princeton University Press, Princeton, New Jersey, 1983). See

also the Lectures at the 1984 Theoretical Advanced Study Institute (Ann Arbor), in *TASI Lectures in Elementary Particle Physics*, edited by David N. Williams (TASI Publications, Ann Arbor, 1984): M. T. Grisaru, p. 232; D. R. T. Jones, p. 284; G. L. Kane, p. 326; P. C. West, p. 365; and the lectures at the 1985 SLAC Summer Institute, contained in *Supersymmetry*, edited by Eileen C. Brennan, SLAC Report No. 296. Other useful references include P. Fayet, in *Proceedings of the 21st International Conference on High Energy Physics*, Paris, 1982, edited by P. Petiau and M. Porneuf [*J. Phys. (Paris) Colloq.* **43**, C3–673 (1982)]; and S. Yamada, in *Proceedings of the 1983 International Symposium on Lepton and Photon Interactions at High Energies*, Ithaca, New York, edited by D. G. Cassel and K. L. Kreinick (Newman Laboratory of Nuclear Studies, Cornell University, Ithaca, 1984), p. 525. The search for supersymmetry in hadron collisions is treated in D. V. Nanopoulos and A. Savoy–Navarro (editors), *Phys. Rep.* **105**, 1 (1984); H. Haber and G. L. Kane, *Phys. Rep.* **117**, 75 (1985); S. Dawson and A. Savoy–Navarro, in *Proceedings of the 1984 Summer Study on Design and Utilization of the Superconducting Super Collider*, edited by R. Donaldson and Jorge G. Morfín (Fermilab, Batavia, Illinois, 1984), p. 263; S. Dawson, E. Eichten, and C. Quigg, *Phys. Rev. D***31**, 1581 (1985).

[55] S. Coleman and J. Mandula, *Phys. Rev.* **159**, 1251 (1967).

[56] R. Haag, J. Łopuszanski, and M. Sohnius, *Nucl. Phys.* **88**, 257 (1975).

[57] In a supersymmetric theory, the supermultiplets are labelled by the chirality of the fermions they contain, and only supermultiplets of the same chirality can have Yukawa couplings to one another. This means that, in contrast to the situation in the standard model, the Higgs doublet which gives mass to the charge 2/3 quarks cannot be the charge conjugate of the Higgs doublet which gives mass to the charge -1/3 quarks, because the charge conjugate of a right-handed (super)field is left-handed. See, for example, S. Weinberg, *Phys. Rev. D***26**, 287 (1982).

[58] R. Barbieri, C. Bouchiat, A. Georges, and P. Le Doussal, *Phys. Lett.* **156B**, 348 (1985).

[59] S. S. Gershtein and Ya. B. Zel'dovich, *Pis'ma Zh. Eksp. Teor. Fiz.* **4**, 174 (1966) [*JETP Lett.* **4**, 120 (1966)]; R. Cowsik and J. McClelland, *Phys. Rev. Lett.* **29**, 669 (1972); B. W. Lee and S. Weinberg, *Phys. Rev. Lett.* **39**, 165 (1977).

[60] H. Goldberg, *Phys. Rev. Lett.* **50**, 1419 (1983); J. Ellis, J. Hagelin, D. V. Nanopoulos, K. Olive, and M. Srednicki, *Nucl. Phys.* **238**, 453 (1984).

[61] W. Bartel, *et al.*(JADE Collaboration), DESY preprint 84–112.

[62] E. Fernandez, *et al.*(MAC Collaboration), *Phys. Rev. Lett.* **54**, 1118 (1985).

[63] G. Bartha, *et al.*, *Phys. Rev. Lett.* **56**, 685 (1986).

[64] N. G. Deshpande, G. Eilam, V. Barger, and F. Halzen, *Phys. Rev. Lett.* **54**, 1757 (1985).

[65] G. Arnison, *et al.* (UA-1 Collaboration), *Phys. Lett.* **166B**, 484 (1986).

[66] J. A. Appel, *et al.* (UA-2 Collaboration), *Z. Phys.* **C30**, 1 (1986).

[67] S. Dawson, in *Supercollider Physics*, edited by D. E. Soper (World Scientific, Singapore, 1986), p. 171.

[68] G. 't Hooft, Ref. 44.

[69] J. Goldstone, *Nuovo Cim.* **19**, 154 (1960).

[70] See S. Coleman and B. Grossman, *Nucl. Phys.* **B203**, 205 (1982) for an investigation of the anomaly condition.

[71] M. Chanowitz and S. D. Drell, *Phys. Rev. Lett.* **30**, 807 (1973).

[72] R. Barbieri, L. Maiani, and R. Petronzio, *Phys. Lett.* **96B**, 63 (1980); S. J. Brodsky and S. D. Drell, *Phys. Rev. D22*, 2236 (1980).

[73] J. Calmet, *et al.*, *Rev. Mod. Phys.* **49**, 21 (1977); F. Combley, F. J. M. Farley, and E. Picasso, *Phys. Rep.* **68**, 93 (1981).

[74] E. Eichten, K. Lane, and M. Peskin, *Phys. Rev. Lett.* **50**, 811 (1983).

[75] J. A. Appel, *et al.* (UA-2 Collaboration), *Phys. Lett.* **160B**, 349 (1985).